



Characteristics, primary sources and secondary formation of water soluble organic aerosols in downtown Beijing

Qing Yu^{1,2}, Jing Chen^{1,2}, Weihua Qin^{1,2}, Siming Cheng^{1,2}, Yuepeng Zhang^{1,2}, Yuewei Sun^{1,2}, Ke Xin^{1,2}, Mushtaq Ahmad^{1,2}

5 ¹State Key Joint Laboratory of Environment Simulation and Pollution Control, School of Environment, Beijing Normal University, Beijing 100875, China.

²Center of Atmospheric Environmental Studies, Beijing Normal University, Beijing 100875, China.

Correspondence to: Jing Chen (jingchen@bnu.edu.cn)

Abstract. Water soluble organic compounds (WSOC) account for a large proportion of aerosols and play a critical role in various atmospheric chemical processes. In order to investigate the primary sources and secondary production of WSOC in downtown Beijing, the day and night PM_{2.5} samples in January (winter), April (spring), July (summer) and October (autumn) of 2017 were collected and analyzed for WSOC and organic tracers in this study. WSOC showed the highest concentration in winter and comparable levels in the other seasons, and dominated by its hydrophobic fraction (HULIS-C). Some typical organic tracers were chosen to evaluate the emission strength and secondary formation for the major sources of WSOC. According to the diurnal patterns and correlation coefficients with the key influencing factors, most SOA tracers were closely related to gaseous photooxidation in summer, but mainly generated via aqueous-phase processing in other seasons. These organic tracers were applied into the positive matrix factorization (PMF) model to calculate the source contributions of WSOC as well as its hydrophobic and hydrophilic portions. The secondary sources contributed over 50 % to WSOC, with higher contributions in summer (75.7 %) and winter (67.7 %), and the largest contributor was aromatic SOC. Besides, the source apportionment results under different pollution levels suggested that controlling biomass burning and the aromatic precursors would be effective to reduce WSOC during the haze episodes in cold seasons. The possible formation mechanisms of the total secondary organic carbon (SOC) as well as hydrophobic and hydrophilic SOC were also explored in this study. The aqueous-phase process appeared to dominate in the SOC formation in winter and spring, while gas-phase photooxidation played a dominant role in summer. Besides, the gaseous photooxidation played a major role in the generation of hydrophobic SOC, whereas aqueous-phase reactions posed vital effects on the formation of hydrophilic SOC.

10
15
20
25



1 Introduction

Organic compounds account for a considerable fraction (20-60 %) of atmospheric aerosols (Huang et al., 2014; Zhang et al., 2020), and water-soluble organic carbon (WSOC) generally takes up 30-70 % of organic carbon (OC) (Zhang et al., 2018; Yang et al., 2019; Chen et al., 2020). WSOC in aerosols is active in light adsorption (Yan et al., 2015; Geng et al., 2020), hence may make significant impact on atmospheric radiative forcing and global climate change (Andreae and Gelencser, 2006). Meanwhile, photoexcitation of water-soluble brown carbon (BrC) can generate oxidants in aerosols and cloud/fog droplets (Manfrin et al., 2019; Kaur et al., 2019), which can promote atmospheric chemical reactions and the aging processes of organic aerosols. Overall, WSOC is extensively involved in the cloud processes and heterogeneous reactions due to its surface activity and water solubility (Ervens et al., 2011; George et al., 2015), thus plays a significant role in severe haze events (Cheng et al., 2015; Wu et al., 2019; Ma et al., 2020). Besides, WSOC is closely linked to the oxidative potential of aerosols, posing adverse health outcomes (Verma et al., 2012; Chen et al., 2019; Wang et al., 2020). Therefore, it is of great significance to study the characteristics, primary sources and secondary production of WSOC in atmospheric particulate matter.

A large fraction of WSOC is formed in the atmosphere, and WSOC greatly overlaps with secondary organic aerosols (SOA) (Zhang et al., 2018). Because most of the organic compounds remain unidentified at the molecular level, it is difficult to thoroughly understand the formation mechanisms of secondary WSOC or SOA. An effective approach to explore the formation mechanisms of SOA is to classify SOA into several categories based on their specific properties. For example, the formation mechanisms of secondary organic carbon (SOC) in the hydrophobic and hydrophilic fractions of WSOC may differ from each other due to their different water-solubility in cloud droplets or the aqueous phase of aerosols. Furthermore, the formation mechanisms may also be different for SOA from different precursors, which originate from various sources and show disparate chemical structures and properties (Sun et al., 2016; Cheng et al., 2018). While gas-phase photooxidation of volatile organic compounds (VOCs) is an important formation pathway of SOA, direct observations have proved that the aqueous-phase reactions of VOCs from biomass burning contribute remarkably to SOA formation (Gilardoni et al., 2016). In this regard, SOA tracers can provide implications for, though may not fully represent, the formation mechanism of SOA from the corresponding precursors.

Humic-like substances (HULIS) have been suggested as the major component of the hydrophobic fraction of WSOC, while short-chain dicarboxylic acids and saccharides are typical hydrophilic WSOC (Miyazaki et al., 2009). Previous studies have revealed that the hydrophobic and hydrophilic fractions of WSOC show significantly different intrinsic oxidative potential, hence would pose different effect on human health (Verma et al., 2012, 2015; Yu et al., 2018). However, source contributions of the hydrophobic and hydrophilic WSOC were scarcely investigated and compared in previous research. So far, the most widely used source apportionment approaches of organic aerosols include the chemical mass balance (CMB)



model coupled with the tracer-yield method (Guo et al., 2012; Islam et al., 2020), and the high-resolution aerosol mass spectrometry combining positive matrix factorization (AMS-PMF) method (Hu et al., 2017; Sun et al., 2018; Shen et al., 2019). The CMB model is used to quantify the primary sources of organic aerosols, while the tracer-yield method is applied to calculate the contributions of secondary sources. However, CMB model requires local source profiles, and the tracer-yield experiments conducted under simple chamber conditions usually ignore the cloud and aqueous-phase processes, leading to large uncertainties when applying these results to the real atmosphere (Kleindienst et al., 2007; Feng et al., 2013). The AMS-PMF method is based on the mass spectra of organic aerosols and massive data analysis, which can avoid such disadvantages. However, the AMS-PMF approach typically classifies secondary organic aerosols into two categories, the less oxidized secondary organic aerosols (LO-OOA) and more oxidized secondary organic aerosols (MO-OOA), which is unable to distinguish SOA from different precursors or sources. To raise effective control measures targeting on specific SOA precursors, recent studies introduced the SOA tracers into PMF model to investigate the secondary sources of WSOC (Kang et al., 2018a, b; Geng et al., 2020). Nevertheless, the respective formation mechanism and sources of the hydrophobic and hydrophilic fractions of WSOC remain unresolved (Verma et al., 2015).

The mean level of $PM_{2.5}$ in Beijing has been greatly reduced since the implement of the Action Plan of Air Pollution Prevention and Control in 2013 (Cheng et al., 2019). Meanwhile, it has been reported that the atmospheric oxidant concentrations were enhanced accompanying the decrease of $PM_{2.5}$ level, which could promote the formation of SOA (Feng et al., 2019). As a result, the sources and composition of WSOC in Beijing would show significant changes due to the control policies implemented in recent years and the enhanced atmospheric oxidizing capacity in the surrounding areas. On the other hand, the haze episodes still occur frequently in Beijing in cold seasons. The humid meteorological conditions as well as the high concentrations of VOC precursors and HONO during haze episodes may pose unique effects on the formation of secondary components in WSOC (Li et al., 2019b; Yang et al., 2019; Zhang et al., 2019). Previous studies found that haze events were usually accompanied with elevated WSOC/OC ratio (Cheng et al., 2015; Yang et al., 2019) and enhanced SOA production (Huang et al., 2014; Li et al., 2019b). Comparison of the formation mechanism and source contributions of WSOC under different pollution levels would help to better understand the complex properties of WSOC, and put forth effective control measures to reduce WSOC during haze events.

In this article, the 12-hour day and night $PM_{2.5}$ samples in Beijing in January, April, July and October of 2017 were collected and analyzed for WSOC and the selected SOA tracers. The chemical characteristics of WSOC and SOA tracers were investigated and the contributions of primary sources and secondary formation to WSOC and its hydrophobic and hydrophilic portions were quantified. In particular, the formation mechanism of the HULIS-C and hydrophilic SOC in WSOC in the four seasons were explored to gain insights into the possible formation mechanism of SOA from different precursors.



90 2. Experimental

2.1 Sampling

Field sampling was performed on the roof of a twenty-meter-high building in the campus of Beijing Normal University in downtown Beijing, which is considered to be a representative urban site. Fine particulate matter ($\text{PM}_{2.5}$) were sampled in four seasons of 2017 by a high-volume sampler with a flow rate of $1.05 \text{ m}^3 \text{ min}^{-1}$, and the sampling periods included January 95 2nd-16th, April 7th-23rd, July 3rd-18th and October 12th -28th in winter, spring, summer and autumn of 2017, respectively. Sampling was conducted during 8:00-19:30 in the daytime and during 20:00-7:30 at night. A total of 124 effective $\text{PM}_{2.5}$ samples were obtained in this study. The field blanks were also collected before and after each sampling duration. All the samples were gathered on the quartz filters (PALLFLEX) which were pre-baked at above 500°C for at least 4 hours before sampling. Before and after sample collections, the quartz filters were weighed by an analytical balance for three times after 100 stabilizing under conditions of fixed temperature ($20 \pm 1^\circ\text{C}$) and humidity ($40 \pm 2\%$) for 24 h. After that, the sampled filters were stored under dark conditions below -20°C until being analyzed.

2.2 Chemical analysis

To measure the values of OC and EC, a part (0.296 cm^2) of each filter was detected using a DRI 2001A carbon analyzer with thermal/optical reflectance (TOR) protocol. The analysis of WSOC and water-soluble ions followed the same procedure as 105 in our previous research (Chen et al., 2014), and the details can be found in the supplementary materials.

WSOC was further divided into the hydrophobic and hydrophilic portions by solid phase extraction (SPE). The hydrophobic fraction of WSOC was directly measured by the following procedure. Briefly, a punch of the sampled filter was shredded into tiny pieces and extracted using 20 mL ultrapure water for a duration of 30 min, and then filtrated via a $0.45 \mu\text{m}$ PTFE filter. The extract was acidified to $\text{pH}=2.0$ with HCl (1 mol L^{-1}), then passed through a SPE cartridge (Oasis HLB, $30 \mu\text{m}$, 110 Waters). After that, the SPE column was rinsed with 3 mL water, then eluted with 1.5 mL MeOH (containing 3 % NH_3) for three times. The eluent was blown to dryness and redissolved in 20 mL water, then measured by a total organic carbon (TOC) analyzer (Shimadzu TOC-L CPN). The hydrophilic WSOC was calculated as total WSOC minus the hydrophobic WSOC.

Seven organic tracers, including levoglucosan, cholesterol, 4-methyl-5-nitrocatechol, phthalic acid (Ph), 2-methylerythritol, 3-hydroxyglutaric acid, and *cis*-pinonic acid (details shown in Section 3.2), were analyzed for each sample in this study. A 115 punch of each filter was ultrasonically extracted twice in 10 mL MeOH for 20 min (below 20°C). The combined extracts were filtrated, concentrated and stored in dark place at -20°C until further derivation. Afterwards, the concentrates were blown to entirely dryness with gentle ultrapure nitrogen (N_2), then redissolved in $100 \mu\text{L}$ pyridine and reacted with $200 \mu\text{L}$ silylating reagent (BSTFA with 1 % TMCS) at 75°C for 70 min. After cooling down to the room temperature, the derivative products were diluted with *n*-hexane and immediately analyzed using the GC/MS/MS equipped with a JA-5MS column. The 120 detailed parameter setting can be found in the supplementary materials. To ensure quality of the measurement, standard



curves with five to seven concentration gradients were re-established every time before the samples were determined. The recovery rates were determined together with ambient samples, by measuring the authentic standards spiked onto the pre-combustioned quartz filters. The recovery rates were all in the range of 70 %-110 %, and the relative standard deviation (RSD) was all below 15 %. The concentrations of the targeted compounds on the field blanks were all close to zero, and the final concentrations reported were all corrected for the blank values.

2.3 PMF source apportionment

PMF 5.0 was applied for the source apportionment of WSOC in PM_{2.5} in four seasons of 2017 with 124 samples. Seventeen species were employed in the PMF model, including WSOC, hydrophobic WSOC, hydrophilic WSOC, elemental carbon, sulfate, nitrate, oxalate, ammonium, magnesium, calcium and seven organic tracers. The uncertainties were calculated referring to the measured RSD data of chemical analysis and previous studies (Kang et al., 2018a). The PMF model was run repeatedly to obtain a clear and reasonable source profile. The Q_{true} and Q_{robust} values of the selected solution agreed well, the distribution of residuals was close to normal with the calculated sum of all species between -3 and +3, and the modeled concentration values correlated strongly ($R^2 > 0.90$) with the measured values, indicating reliability of the selected PMF solution.

2.4 Other data collection and calculations

During the sampling periods, the meteorological parameters were simultaneously monitored using a HOBO meteorological station at our sampling site. The hourly concentrations of O₃ and CO were obtained from a nearby urban air monitoring station (3.4 km from the sampling site) via the website at <http://www.bjmemc.com.cn>. These data were transformed to 12-h averages corresponding to the sampling time.

The aerosol acidity was estimated by the molar ratio of major anions to cations in aerosols (Fu et al., 2015): $R_{A/C} = ([Cl^-] + [NO_3^-] + 2[SO_4^{2-}] + 2[C_2O_4^{2-}]) / ([NH_4^+] + [K^+] + [Na^+] + 2[Ca^{2+}] + 2[Mg^{2+}])$.

The liquid water content (LWC) in inorganic aerosols was calculated by the ISORROPIA-II model (Fountoukis and Nenes, 2007), and the reverse mode was chosen in this study since the concentrations of gaseous pollutants such as HCl, HNO₃ and NH₃ were not available here. The total aerosol LWC was the summation of the water in both water-soluble ions and organic species, and the latter was calculated by the approach described by Cheng et al. (2016).

The OC emission amounts from open biomass burning over the sampling periods in the four seasons of 2017 were obtained from the Fire Inventory (FINNv1.5), which provides daily estimates of OC emissions from wildfire and agricultural fires with a resolution of 1 km (Wiedinmyer et al., 2011), and processed by the fire_emis utility provided on <http://bai.acom.ucar.edu/Data/fire/>. The values of OC emissions in the Beijing-Tianjin-Hebei region were extracted by the Geographic Information System (GIS).



3 Results and discussion

3.1 Temporal trends of carbonaceous species

The temporal variations of WSOC, OC, EC and PM_{2.5} over the study periods in the four seasons of 2017 are presented in Fig. 1, and their average concentrations are summarized in Table 1. In general, the carbonaceous species exhibited similar variation trends with that of PM_{2.5} throughout the whole sampling period, which approximately varied in periodic cycles of two to seven days (Guo et al., 2014). The average values of WSOC, OC, EC and PM_{2.5} in winter were all much higher than in other seasons. The mean levels of OC, EC and PM_{2.5} were in the descending order of autumn > spring > summer, while WSOC showed comparable levels in these three seasons. The fact that WSOC showed mild temporal variation with no sudden increase in autumn implied that short-term outdoor biomass burning after the harvest season in the surrounding areas of Beijing was well controlled over the sampling period in autumn. As shown in Table S1, the OC concentration in PM_{2.5} in Beijing exhibited an overall declining trend in the past ten years, but WSOC showed no obvious change. Therefore, the control of WSOC seemed to be more challenging compared to the control of water-insoluble organic aerosols.

The temporal variation of the WSOC/OC ratio is also illustrated in Fig. 1. WSOC/OC showed the highest average value in summer, followed by winter. The range of WSOC/OC in this study was similar to that previously reported in urban Beijing (Zhao et al., 2018; Yang et al., 2019), except for the significantly decreased ratio in autumn. This might be owing to the effective control of the open burning of crop residues in the surrounding areas in recent years. Previous research showed that the aggravation of PM_{2.5} pollution was usually accompanied by the elevated WSOC/OC ratio (Cheng et al., 2015; Yang et al., 2019), which was also confirmed by the significant positive relationships between PM_{2.5} and WSOC/OC in the four seasons (winter: $r=0.68$, $p<0.01$; spring: $r=0.61$, $p<0.01$; summer: $r=0.36$, $p<0.05$; autumn: $r=0.91$, $p<0.01$) in this study, again underlining the important role of WSOC in the haze evolution process. In this work, WSOC was further divided into its hydrophobic and hydrophilic portions. As listed in Table 1, the hydrophobic portion dominated in the total WSOC in all seasons, and also exhibited the highest proportion in summer (0.84), followed by winter (0.73), higher than the results previously reported in Beijing (Li et al., 2019a; Huang et al., 2020). The ratio of hydrophilic WSOC to total WSOC showed significant positive correlations with PM_{2.5} in winter ($r=0.58$, $p<0.01$), summer ($r=0.48$, $p<0.05$) and autumn ($r=0.44$, $p<0.05$), implying that the organic aerosols became more hygroscopic as pollution aggravated in these seasons (Guo et al., 2014).

3.2 Characteristics of organic tracers

3.2.1 Seasonal variations and diurnal patterns

In order to reveal the emission strength and secondary formation of WSOC, the characteristics of typical organic tracers were investigated. The mean values of organic tracers identified in this study are shown in Table 1. Levoglucosan is an ideal tracer for biomass burning, while cholesterol is a good indicator of cooking, and both of them are known as primary organic



tracers. Previous research have shown that phthalic acid can be used as the aromatic SOA tracer (Al-Naiema and Stone, 2017; Huang et al., 2019), while 4-methyl-5-nitrocatechol is a good indicator for biomass burning SOA (Iinuma et al., 2010; Amelie et al., 2018), and both of them serve as anthropogenic SOA tracers. The biogenic SOA tracers under study included isoprene SOA tracer 2-methylerythritol, as well as *cis*-pinonic acid and 3-hydroxyglutaric acid, which are lower- and higher-generation oxidative products of monoterpenes respectively (Kourtchev et al., 2009). To eliminate the influence of atmospheric diffusion and better clarify the differences in emission strength or secondary production rate in different seasons, the concentrations of these organic tracers were divided by the level of carbon monoxide (CO), which has constant emission rate and is inert to chemical reactions. Seasonal variations of their CO-scaled concentrations and the day to night ratios are presented in Fig. 2.

Primary organic tracers. The average CO-scaled concentration of levoglucosan in summer was much lower than in the other three seasons (only 15.4 % of that in winter), suggesting that biomass burning was not active in summer (Sun et al., 2018; Duan et al., 2020). Levoglucosan exhibited similar CO-scaled concentrations in seasons other than summer, indicating that the emission strength from biomass burning was relatively constant in these seasons and open burning of crop residues, which has distinct seasonality, was not a significant source of levoglucosan. The OC emission from open biomass burning in the Beijing-Tianjin-Hebei region as provided by the Fire Inventory were 302 Mg (winter), 1557 Mg (spring), 1818 Mg (summer) and 501 Mg (autumn), respectively. The OC emission from open biomass burning showed completely different seasonal distribution pattern from that of levoglucosan, which further proved that open biomass burning was not the major source of levoglucosan. Residential biofuel combustion (Chen et al., 2017) as well as coal combustion (Yan et al., 2018) might be the main sources of levoglucosan in Beijing. The day/night ratio of the CO-scaled concentration of levoglucosan was lower than 1 except in winter, implying stronger nighttime primary biomass burning emissions in Beijing except in winter (Yan et al., 2019). The CO-scaled concentration of cholesterol was close in the whole sampling period, indicating that the cooking emission was relatively constant throughout the year (Sun et al., 2018).

Anthropogenic SOA tracers. Phthalic acid exhibited the highest CO-scaled concentration in winter, followed by summer, reflecting stronger secondary production of aromatic SOA in these two seasons (Ding et al., 2017). In winter, the enhanced emissions due to the heating activities together with the adverse atmospheric diffusion conditions resulted in higher concentrations of aromatic precursors, which consequently facilitated the secondary formation of aromatic SOA (Feng et al., 2018; Sun et al., 2018). In comparison, the second highest value of phthalic acid occurring in summer was probably due to high temperature and relative humidity, strong solar radiation and abundant atmospheric oxidants in summer, which was favorable for secondary photochemical reactions (Zhao et al., 2018). The day/night ratio of phthalic acid was higher than 1 in all four seasons, implying that the photochemical reactions contributed to the secondary formation of aromatic SOA all the year round (Kawamura and Yasui, 2005). The ratio in summer was much higher than in the other seasons, implying more prominent effects of the photochemical processes on the generation of aromatic SOA in summer. 4-Methyl-5-nitrocatechol was generally below the detection limit for the summer samples, again indicating negligible biomass burning emissions in



215 summer. It is notable that the CO-scaled value of 4-methyl-5-nitrocatechol in winter was much higher than that in spring and
autumn (Kahnt et al., 2013), while the primary emission intensity of biomass burning was relatively constant in these three
seasons as revealed by the seasonal distribution pattern of levoglucosan. This phenomenon can be explained by the following
reasons. Firstly, the worse diffusion conditions in winter favored the accumulation of the precursors such as phenols and
NO_x (Iinuma et al., 2010), and the secondary formation rate of biomass burning SOA increased consequently. Secondly, the
220 low temperature and high aerosol LWC in winter were beneficial for the partitioning of gaseous phenols to the aerosol phase.
Besides, the high concentration of HONO in winter might contribute to the generation of nitrocatechols in the condensed
phase (Kristija et al., 2018; Qu et al., 2019). Therefore, the aqueous-phase or heterogeneous reactions were enhanced (Li et
al., 2014; Gilardon et al., 2016). Similar to levoglucosan, the day/night ratio of 4-methyl-5-nitrocatechol was all less than 1
in the four seasons (Gaston et al., 2016; Wang et al., 2019), again indicating stronger biomass burning emissions at night. As
225 illustrated in Fig. 2, the day to night ratio of 4-methyl-5-nitrocatechol was even lower than that of levoglucosan, which was
partly attributable to the stronger aqueous-phase reactions at night with higher LWC and precursor concentrations (Wang et
al., 2019). Furthermore, the dark formation of methyl-nitrocatechols might also exist at night in the presence of HONO
(Kristijan et al., 2018).

Biogenic SOA tracers. As shown in Fig. 2., 2-methylerythritol and 3-hydroxyglutaric acid exhibited extremely high CO-
230 scaled concentrations in summer, followed by spring and autumn, and showed the minimum concentrations in winter. The
mean concentration of 2-methylerythritol in summer was almost 50 times of that in winter. Such seasonal variations of
biogenic SOA tracers indicated much stronger biogenic SOA generation in summer, which was attributable to the higher
emissions of biogenic precursors and accelerated photochemical reactions (Shen et al., 2015; Qiu et al., 2020). Nevertheless,
cis-pinonic acid, another monoterpene SOA tracer, exhibited slightly higher CO-scaled concentration in spring than in
235 summer. The active atmospheric oxidation processes in summer might facilitate the transformation of *cis*-pinonic acid to the
higher-generation oxidation products. In addition, *cis*-pinonic acid tends to evaporate into the gas phase in summer under
high temperature (Li et al., 2013; Ding et al., 2016). For the same reason, the day/night ratio of *cis*-pinonic acid in summer
was significantly lower than the ratio in other seasons. The diurnal patterns of 2-methylerythritol and 3-hydroxyglutaric acid
were similar and close to 1 in the four seasons, indicating that the formation pathway through photochemical oxidation for
240 these two biogenic SOA tracers was not as important as for phthalic acid. The lower day/night ratio of 2-methylerythritol in
spring and autumn was likely associated with the elevated amount of isoprene from biomass burning activities at night
(Akagi et al., 2011), which was further confirmed by the strong correlation between 2-methylerythritol and levoglucosan in
these two seasons (spring: $r=0.71$, $p<0.01$; autumn: $r=0.77$, $p<0.01$).

3.2.2 Influence factors and speculative production pathways of different SOA tracers

245 In order to better understand the possible formation pathways of the SOA tracers of different sources, the Spearman
correlation analysis was conducted between the SOA tracers as well as WSOC/OC and the meteorological parameters, O₃,



aerosol acidity and aerosol liquid water content (LWC). The correlation analysis results are shown in Table S2 and Fig. 3. As listed in Table S2, WSOC/OC did not appear any correlation with O_3 or solar radiation ($p > 0.05$) in each sampling period, suggesting that gas-phase photooxidation was not the dominant formation mechanism of SOC. The WSOC/OC ratio correlated strongly with RH, LWC and aerosol acidity in seasons other than summer, indicating that acid-catalyzed aqueous-phase reactions might be the dominant formation pathway of SOC in these seasons (Du et al., 2014; Yang et al., 2019). Besides, the increased LWC could also facilitate the partitioning of gas-phase WSOC to the condensed phase (Hennigan et al., 2009), resulting in a higher WSOC/OC ratio. No such correlations were found in summer, probably due to the enhanced gas-phase photochemical oxidation in SOC formation in summer. In autumn and winter with lower temperature, the WSOC/OC ratio significantly correlated with temperature (autumn: $r = 0.47$, $p < 0.01$; winter: $r = 0.50$, $p < 0.01$), while in spring and summer when the weather became warmer, no significant correlations were found between them. Higher temperature in warm seasons might inhibit the gas-to-particle partition of semi-volatile or intermediate WSOC and the related heterogeneous reactions (Qian et al., 2019; Lu et al., 2019), thus counteracting its promoting effect on SOC formation. The correlation pattern of individual SOA tracers with the influencing factors, which is distinct from that of WSOC/OC, is discussed hereinafter.

As illustrated in Fig. 3, the biomass burning SOA tracer, 4-methyl-5-nitrocatechol, showed strong positive relationships with relative humidity, LWC and aerosol acidity, and strong negative relationships with O_3 concentration and solar radiation in winter and spring. The correlations with the above parameters became weaker in autumn and no data was available in summer because 4-methyl-5-nitrocatechol was below the detection limit. Laboratory studies have shown that phenolic compounds, which are massively emitted from biomass burning, could undergo rapid aqueous-phase oxidation and produce substantial amounts of SOA under either the simulated sunlight (Sun et al., 2010; Li et al., 2014; Yu et al., 2014) or the dark conditions (Hartikainen et al., 2018; Kristijan et al., 2018). Direct observations have also proved that the aqueous-phase reactions of the precursors from biomass burning emissions contribute significantly to SOA formation (Gilardoni et al., 2016). Therefore, the correlation results together with the literature findings indicated that the contributions of gaseous photochemical reactions were negligible for the formation of 4-methyl-5-nitrocatechol in winter and spring, while the acid-catalyzed aqueous-phase reactions were the principle generation pathway of 4-methyl-5-nitrocatechol (Wang et al., 2019). The reverse relationship with temperature in spring and autumn was probably because that the increasing temperature was conducive to the evaporation of phenolic species thus could inhibit the secondary production of 4-methyl-5-nitrocatechol via the aqueous-phase reactions.

The aromatic SOA tracer, phthalic acid, showed different formation pathways in different seasons. Chamber studies have revealed that the enhanced aerosol LWC could significantly increase the yields of aromatic SOA (Jia and Xu, 2018; Lu et al., 2019; Zhou et al., 2019). In this study, phthalic acid showed significant positive relationships with RH, LWC and aerosol acidity in seasons other than summer, suggesting that acid-catalyzed aqueous-phase reactions were also the major formation pathway of the aromatic SOA in these seasons. Phthalic acid showed significant positive relationship with O_3 and significant



negative association with RH in summer, indicating that the photochemical processes played a major role in aromatic SOA formation in summer (Kawamura and Yasui, 2005). Phthalic acid showed significant positive correlation with temperature in summer ($r=0.71$, $p<0.01$), affirming the promoting impact of temperature on the gas-phase photochemical processes.

The isoprene SOA tracer, 2-methylerythritol, could be formed through the gas-phase reaction with $\cdot\text{OH}$ radical (Claeys et al., 2004a) and acid-catalyzed heterogeneous oxidation with H_2O_2 (Claeys et al., 2004b). In addition, it can also be formed by reactive uptake of the isoprene-derived epoxydiols (IEPOX) generated in the gaseous phase and subsequent aqueous-phase processing (Surratt et al., 2010; Xu et al., 2015). During the whole sampling period, 2-methylerythritol showed significantly positive relationships with temperature ($r=0.60$, $p<0.01$), RH ($r=0.55$, $p<0.01$), O_3 ($r=0.33$, $p<0.01$), aerosol acidity ($r=0.80$, $p<0.01$) and LWC ($r=0.56$, $p<0.01$), suggesting that both the gas-phase photooxidation and aqueous-phase reactions played significant roles in the formation of 2-methylerythritol. 2-Methylerythritol was mainly formed by gas-phase photooxidation in summer, while it was more closely associated with the aqueous-phase reactions in the other seasons, particularly in winter. 2-Methylerythritol did not correlate significantly with temperature in winter, spring or autumn, however, when the temperature was above 25°C , it grew rapidly as temperature increased, similar to the results found in the previous research (Liang et al., 2012).

The monoterpene SOA tracer, 3-hydroxyglutaric acid appeared significant positive relationships with temperature ($r=0.63$, $p<0.01$), RH ($r=0.53$, $p<0.01$), O_3 ($r=0.37$, $p<0.01$), aerosol acidity ($r=0.77$, $p<0.01$) and LWC ($r=0.58$, $p<0.01$) over the whole sampling duration (Table S2), which suggests that gas-phase photooxidation and aqueous-phase reactions were both important for the formation of 3-hydroxyglutaric acid. Besides, 3-hydroxyglutaric acid correlated strongly with 2-methylerythritol ($r=0.94$, $p<0.01$), implying similar formation mechanisms for the two biogenic SOA tracers. According to the correlation coefficients shown in Table S2 and Fig. 3, the major formation mechanism of 3-hydroxyglutaric acid was gaseous photooxidation in summer, and aqueous-phase processing in both winter and spring, while the linkage to the aqueous-phase processes might be slightly weaker in autumn. The correlation pattern of another biogenic SOA tracer, *cis*-pinonic acid, seemed to be different from that of 3-hydroxyglutaric acid and 2-methylerythritol. Chamber studies have shown that *cis*-pinonic acid could be produced by the gas-phase reactions of monoterpenes (Yu et al., 1999; Larsen et al., 2011), which highly contributes to newly nucleated particles (Zhang et al., 2011). Field observations also found that *cis*-pinonic acid was closely associated with nucleation processes as the first step in the production of SOA from organic vapors (Alier et al. 2013; van Drooge et al., 2018). However, no significant correlations were found between *cis*-pinonic acid and temperature or O_3 in summer, possibly because it is an unstable intermediate and can further generate higher-generation products such as 3-hydroxyglutaric acid (Kourtchev et al., 2009). Similar to the other SOA tracers, *cis*-pinonic acid displayed significant positive relationships with RH, LWC and aerosol acidity in winter, possibly because the higher RH and aerosol acidity in winter could enhance the reactive uptake and heterogeneous reactions of the gas-phase pinonaldehyde, the precursor of *cis*-pinonic acid (Liggio et al., 2006; Larsen et al., 2011; Zhao et al., 2013).



3.3 Primary sources and secondary generation of WSOC

3.3.1 Source apportionment of WSOC

Source apportionment of PMF was conducted to investigate the source contributions of WSOC as well as its hydrophobic and hydrophilic fractions. Nine types of sources were identified in this study as shown in Fig. 4. Source 1 showed high levels of levoglucosan and EC, thus was interpreted as direct emissions of biomass burning. Source 2 had a high level of cholesterol, hence was identified as cooking. Source 3 exhibited a large fraction of EC which can not be explained by the direct emissions of biomass burning, implying that it was the direct emissions of other combustion sources. Source 4 was characterized by high fractions of Mg^{2+} and Ca^{2+} , thus was considered as dust. No significant EC but high proportions of 4-methyl-5-nitrocatechol and phthalic acid were observed in Source 5 and Source 6, respectively, which were recognized to be SOC from biomass burning (biomass burning SOC) and aromatic precursors (aromatic SOC), respectively. Source 7 exhibited a high level of *cis*-pinonic acid, thus was explained as freshly generated biogenic SOC. Source 8 was featured by high fractions of 2-methylerythritol and 3-hydroxyglutaric acid, which are the end products from isoprene and monoterpenes respectively, hence was identified as aged biogenic SOC. Note that 3-hydroxyglutaric acid and *cis*-pinonic acid were not grouped into one source though they are both the SOA tracers of monoterpenes, owing to their different reactivity as discussed above. Source 9 covered secondary components (such as SO_4^{2-} , NO_3^- , NH_4^+ and $C_2O_4^{2-}$) that can not be well explained by the identified sources above, thus was considered to be SOA from other sources.

Source contributions to the total WSOC as well as its hydrophobic and hydrophilic fractions are illustrated in Fig. 5. During the whole sampling period, the primary emissions of biomass burning contributed 23.0 % to the total WSOC, with a higher contribution to its hydrophilic fraction (37.2 %) than to the hydrophobic section (15.7 %), which was probably due to the large amounts of saccharides with high water-solubility from biomass burning (Yan et al., 2019; Xu et al., 2020). The total contribution of primary and secondary biomass burning to WSOC (35.3 %) was slightly lower than that previously reported in Beijing (Cheng et al., 2013; Li et al., 2018; Duan et al., 2020), likely owing to the effective control of the open biomass burning activities in the surrounding areas of Beijing in recent years. Other primary combustion sources (Source 3) also contributed considerably to WSOC (14.4 %), most of which only contributed to the hydrophobic fraction (19.1 %). Recent source apportionment based on CMAQ model in North China reported that coal combustion contributed 15.1 % to water-soluble HULIS (HULISws) annually, which is the major component of hydrophobic WSOC (Li et al., 2019a). High levels of HULISws were also observed in the coal combustion smoke, again suggesting that coal combustion might be a significant source of HULISws (Fan et al., 2016). However, Source 3 did not show the highest contribution in winter when domestic heating required extra combustion amounts of coal, implying that there could be other sources except for coal combustion contributing to hydrophobic WSOC. Previous studies using PMF analysis also revealed that traffic and waste burning both contributed more than 15 % to HULISws in Beijing (Ma et al., 2018; Li et al., 2019c). Therefore, the mixed primary sources in Source 3 possibly consisted of coal combustion, traffic emission, waste incineration, etc. Previous AMS studies in Beijing indicated that cooking contributed more than 10 % to total organic aerosols (Hu et al., 2016; Sun et al., 2018; Duan et al.,



2020). However, the contribution of cooking to WSOC was quite low (1.5 %) in this study, probably because it contributed more significantly to the water-insoluble fraction of organic aerosols (Zhao et al., 2007). Our results also showed that cooking only contributed to the hydrophobic fraction of WSOC. Dust contributed 7.0 % to WSOC, with 4.0 % to the hydrophobic fraction and 12.9 % to the hydrophilic fraction. The difference between the hydrophilic and hydrophobic fractions might be explained by the hydrophilic fulvic acids from soil resuspension and the hydrophilic saccharides carried by dust (Li et al., 2018).

As shown in Fig. 5 (a), the secondary sources contributed 54.1 % to total WSOC, slightly higher than the results of Cheng et al. (2013) and Tao et al. (2016) and similar to the result of Du et al. (2014). The secondary sources exhibited a higher contribution to hydrophobic WSOC (57.8 %) than hydrophilic WSOC (45.3 %). The aromatic SOC was the most abundant secondary source of WSOC (26.6 %) as well as its hydrophobic (24.1 %) and hydrophilic fractions (30.9 %) in urban Beijing (Tang et al., 2018). Biogenic SOC (12.4 %) and biomass burning SOC (12.3 %) contributed comparable proportions to total WSOC, and both contributed more to the hydrophobic fraction. Biomass burning SOC, which is mainly formed from the phenolic compounds, has been widely recognized to contribute notably to the water-soluble brown carbon (HULIS_{WS}) (Smith et al., 2016; Pang et al., 2020). Biogenic SOC in the hydrophilic fraction (contribution ratio of aged to fresh: 1.44) was more aged than that in the hydrophobic fraction (contribution ratio of aged to fresh: 0.54), because the atmospheric aging processes would generally increase the polarity of organic aerosols (Baduel et al., 2011; Guo et al., 2014).

3.3.2 Seasonal variations of source contributions

The seasonal variations of the source contributions to total WSOC and its hydrophobic and hydrophilic fractions are presented in Fig. 5(b). WSOC was mainly derived from the secondary sources in summer (75.7 %) and winter (67.7 %), but dominated by the primary emissions in spring (68.1 %) and autumn (70.8 %), similar to that of Qiu et al. (2020). In winter, WSOC mainly originated from the anthropogenic sources (Li et al., 2018; Zhang et al., 2018), including the aromatic SOC (37.2 %), biomass burning SOC (28.3 %), and primary biomass burning (20.8 %). The significant contributions of anthropogenic SOC in winter probably resulted from the stronger emissions of aromatic precursors and phenolic compounds from the domestic heating activities such as household combustion of solid fuels (Liu et al., 2016). The meteorological conditions during the sampling period in winter (slow wind speed, low temperature and high relative humidity) also favored the accumulation and heterogeneous uptake of the SOC precursors, leading to stronger SOC production. It is therefore crucial to control biomass burning and the aromatic precursors to reduce WSOC in winter. In summer, the largest contributor to WSOC was biogenic SOC (42.9 %) that was highly oxidized, in consistent with the higher O/C ratio found in summer in previous research (Hu et al., 2016; Xu et al., 2017; Qiu et al., 2020). Aromatic SOC (28.0 %) also contributed significantly to WSOC in summer, as reported previously in the summer of urban Beijing (Guo et al., 2012). Unlike the case in winter with stronger anthropogenic emissions and stagnant and humid meteorological conditions, the high fraction of aromatic SOC in summer was largely associated with the stronger photooxidation capacity. Both primary and secondary contributions from



biomass burning were negligible in summer. Nevertheless, the direct emissions from biomass burning contributed the highest to WSOC in both spring (27.4 %) and winter (42.8 %), with much greater contributions to the hydrophilic WSOC than the hydrophobic WSOC in both seasons. Besides, in the spring season when the weather was windy and dusty, dust showed the highest contribution (22.1 %) to WSOC among the four seasons. The contribution of fresh biogenic SOC (14.9 %) was significantly enhanced in spring compared to that in winter as temperature gradually increased, while the contribution of aromatic SOC (17.3 %) decreased dramatically compared to that in winter due to the cessation of the heating activities (Yu et al., 2019).

As shown in Fig. 1 as well as in previous studies, winter and autumn in North China Plain are the two seasons that endure more severe air pollution and show higher concentrations of PM_{2.5}. Therefore, the source contributions to WSOC in PM_{2.5} in winter and autumn under different pollution levels were also investigated, as shown in Fig. 6. In winter, both the primary and secondary contributions from biomass burning increased significantly from clean days to moderate hazy days, while the aromatic SOC and biomass burning SOC dominated over severe hazy days (Zhang et al., 2018), highlighting the important roles of biomass burning and aromatic SOC during the hazy periods in winter (Elser et al., 2016; Li et al., 2017; Huang et al., 2019; Yu et al., 2019). In autumn, both the contributions of aromatic SOC and biomass burning SOC gradually increased as the haze conditions aggravated. Meanwhile, the fresh biogenic SOC became less important with the aggravation of the haze conditions, which might be due to the inhibited gas-phase photochemical oxidation as discussed above. Again, the change of source contributions in winter and autumn under different pollution levels suggested that the control of biomass burning and reduction of the aromatic precursors would be of great significance for controlling WSOC in hazy days.

3.3.3 Exploratory formation mechanisms of hydrophobic and hydrophilic SOC

As the secondary sources contributed highly to both the hydrophobic (57.8 %) and hydrophilic WSOC (45.3 %), the formation mechanisms of the secondary proportions of the hydrophobic and hydrophilic WSOC were explored and compared. Fig. 7(a) shows the RH versus O₃ dependence of the ratios of hydrophobic SOC/OC, hydrophilic SOC/OC, and hydrophilic SOC/hydrophobic SOC during the whole sampling period. Both of the ratios of hydrophobic SOC/OC and hydrophilic SOC/OC increased with O₃ and RH, suggesting that both gas-phase photooxidation and aqueous-phase reactions played a critical role in the production of hydrophobic and hydrophilic SOC. Compared to the hydrophilic SOC, the hydrophobic SOC/OC ratio was more dependent on O₃ ($r=0.31$, $p<0.01$), and exhibited significantly higher values during the daytime (Nonparametric test, $p<0.05$), emphasizing the more critical role of photooxidation in the formation of hydrophobic SOC. Laboratory studies showed that the photo-induced auto-oxidation of PAHs could lead to the production of HULISws that can not be formed under dark conditions (Haynes et al., 2019). Besides, the photo-induced oligomerization of some phenolic compounds could also form HULISws (Vione et al., 2019). Field observations reported an obviously higher contribution of the ultrafine aerosol mode to the hydrophobic WSOC in summer, which suggested that the formation of the hydrophobic SO was tightly associated with the gaseous phase nucleation (Frka et al., 2018). In comparison, the ratio of



hydrophilic SOC/OC was more sensitive to RH ($r=0.41$, $p<0.01$) than to O_3 ($p>0.05$), implying the significant effect of the aqueous-phase processing on the formation of hydrophilic SOC. Quantum chemical calculations in a recent study also indicated that the carbenium ion-mediated reactions that involve highly hydrophilic organic compounds occur efficiently in weakly acidic aerosols and cloud/fog droplets, contributing significantly to SOC generation (Ji et al., 2020). The hygroscopicity of organic aerosols increased with their aging degree through their evolution processes (Jimenez et al., 2009; Wu et al., 2016; Kuang et al., 2020), therefore, the ratio of hydrophilic SOC/hydrophobic SOC was employed to indicate the aging degree of SOC. The ratio of hydrophilic SOC/hydrophobic SOC showed a strong dependence on RH ($r=0.61$, $p<0.01$), indicating that the aqueous-phase oxidation played a crucial role in the aging processes of SOA. Previous research using high resolution AMS also indicated that the ambient SOA was usually more oxidized than those generated in dry smog chambers in which SOA could only be produced through the gas-phase oxidation (Aiken et al., 2008), and such discrepancy could be explained by the aqueous-phase processing that produced more hydrophilic SOA (Ervens et al., 2011). Previous research on the aging processes in fog droplets and aerosols also supported the finding that the aqueous-phase reactions can lead to the generation of more oxidized and hydrophilic SOA (Brege et al., 2018).

To further investigate the generation mechanism of the hydrophobic and hydrophilic SOC in different seasons, correlation coefficients between the above ratios and some meteorological parameters, O_3 , $PM_{2.5}$, the aerosol acidity and aerosol LWC in the four seasons are illustrated in Fig. 7 (b). In winter, both the ratios of hydrophobic SOC/OC and hydrophilic SOC/OC exhibited strong positive relationships with RH, aerosol acidity and LWC, suggesting that acid-catalyzed heterogeneous reactions were the dominant secondary formation mechanism of both the hydrophobic and hydrophilic SOC in winter. Such result was in consistent with the previous finding that the aqueous-phase oxidation dominated in winter when the gaseous photochemical oxidation was usually weak (Duan et al., 2016; Wu et al., 2019; Yu et al., 2019). In spring, the SOC/OC ratio also exhibited significant positive relationships with RH ($r=0.45$, $p<0.01$), aerosol acidity ($r=0.63$, $p<0.01$) and aerosol LWC ($r=0.44$, $p<0.05$), but lower than those in winter (RH: $r=0.67$, $p<0.01$; aerosol acidity: $r=0.82$, $p<0.01$; LWC: $r=0.84$, $p<0.01$). In summer, the SOC/OC ratio exhibited significantly positive relationships with O_3 ($r=0.45$, $p<0.05$) and temperature ($r=0.55$, $p<0.01$), implying that the photooxidation process was the major formation pathway of SOC, possibly due to the stronger solar radiation in summer (Tang et al., 2016; Duan et al., 2020). However, the aqueous-phase process still played an important role in transforming the less oxidized hydrophobic SOC to the more oxidized hydrophilic SOC based on the significant correlations between the ratio of hydrophilic SOC to hydrophobic SOC and LWC ($r=0.60$, $p<0.01$). In autumn, similarly based on the correlation pattern of the respective ratio with the influencing factors, the production of hydrophobic SOC showed a stronger linkage to the photooxidation process, while the aqueous-phase reactions played a more critical role in the formation of hydrophilic SOC and the aging processes of SOA. Besides, the SOC/OC ratio exhibited significant positive relationships with $PM_{2.5}$ in winter ($r=0.84$, $p<0.01$), spring ($r=0.47$, $p<0.01$) and autumn ($r=0.52$, $p<0.01$), reflecting the enhanced SOC formation as pollution aggravated in these seasons (Zhang et al., 2014; Li et al., 2019b). However, no



such relationship between SOC and PM_{2.5} was found in summer ($r=0.03$, $p>0.05$) when the gaseous photooxidation dominated in the SOC formation.

4 Conclusions

Based on the WSOC and related SOA tracer analysis for the PM_{2.5} samples collected in downtown Beijing in different seasons of 2017, HULIS-C, or the hydrophobic fraction of WSOC dominated in WSOC during the whole sampling period, which showed the highest proportion to WSOC in summer. However, the organic aerosols became more hygroscopic as pollution aggravated and the ratio of hydrophilic WSOC to total WSOC increased with PM_{2.5} in seasons other than summer. Compared to the previous studies in Beijing over the past decades, the reduction of WSOC in this study was not as obvious as that of OC, indicating that the control of WSOC is a more challenging task than the control of water-insoluble organics.

The secondary sources contributed more than 50 % to WSOC, with higher contributions in summer (75.7 %) and winter (67.7 %) than in spring (31.9 %) and autumn (29.2 %). Aromatic SOC (26.6 %) was the most abundant secondary source over the entire study period. Biomass burning SOC played a significant role (28.3 %) in winter, while biogenic SOC showed the highest contribution (42.9 %) in summer. The primary emissions of biomass burning and other primary combustion sources were the major primary sources of hydrophobic WSOC, while the hydrophilic WSOC was largely affected by the primary emissions of biomass burning and dust. The combined contribution of primary and secondary biomass burning to WSOC was slightly lower than that previously reported in Beijing owing to the effective control of open burning in the surrounding areas. Nevertheless, the contributions of biomass burning SOC and aromatic SOC to WSOC obviously increased as pollution aggravated in the haze periods in winter and autumn, suggesting that the control of biomass burning and reduction of the aromatic precursors would be of great significance for controlling WSOC during severe haze episodes.

According to the correlation patterns with the key influencing factors of the gas phase and aqueous phase reactions, the acid-catalyzed aqueous-phase processing was suggested as the major formation pathway of SOC in winter and spring, while the gas-phase photooxidation played a critical role in summer. The gaseous photooxidation played a more prominent role in the formation of hydrophobic SOC, whereas the aqueous-phase processing posed more profound effects on the formation of hydrophilic SOC and the aging processes of SOC. The SOA modeling based on the chemical transport models has been a powerful tool for the SOA study in regional scale. However, the SOA modeling remains a challenge and model studies have shown systematically underestimated ambient SOA concentrations compared to the observed values. The findings of this study would help to reduce the model-measurement discrepancies of SOA by underlining the importance of the SOA properties and the contributions of heterogeneous formation processes in different seasons.



470 Data availability.

The data used in this article are available from the authors upon request (jingchen@bnu.edu.cn).

Author contribution

The corresponding author, JC, provided the ideas and funding, discussed the results, and revised the paper. The first author QY conducted the sampling and chemical analysis, analyzed the data, plotted the figures, and wrote the manuscript. WhQ, SmC, YpZ, YwS, KX, MA contributed to the field sampling and put forward suggestions on the discussion. WhQ and YpZ
475 helped with the data processing from FINNv1.5.

Competing interests.

The authors declare that they have no conflict of interest.

References

- 480 Aiken, A. C., Decarlo, P. F., Kroll, J. H., Worsnop, D. R., Huffman, J. A., Docherty, K. S., Ulbrich, I. M., Mohr, C., Kimmel, J. R., Sueper, D., Sun, Y., Zhang, Q., Trimborn, A., Northway, M. J., Ziemann, P., Canagaratna, M. R., Onasch, T. B., Alfarra, M. R., Prevot, A. S. H., Dommen, J., Duplissy, J., Metzger, A., Baltensperger, U., and Jimenez, J. L.: O/C and OM/OC ratios of primary, secondary, and ambient organic aerosols with high-resolution time-of-flight aerosol mass spectrometry, *Environ. Sci. Technol.*, 42, 4478-4485, doi:10.1021/es703009q, 2008.
- 485 Akagi, S. K., Yokelson, R. J., Wiedinmyer, C., Alvarado, M. J., Reid, J. S., Karl, T., Crounse, J. D., and Wennberg, P. O.: Emission factors for open and domestic biomass burning for use in atmospheric models, *Atmos. Chem. Phys.*, 11, 4039-4072, doi:10.5194/acp-11-4039-2011, 2011.
- Alier, M., van Drooge, B. L., Dalosto, M., Querol, X., Grimalt, J. O., and Tauler, R.: Source apportionment of submicron organic aerosol at an urban background and a road site in Barcelona (Spain) during SAPUSS, *Atmos. Chem. Phys.*, 13, 10353-10371, doi:10.5194/acp-13-10353-2013, 2013.
- 490 Al-Naiema, I., and Stone, E.: Evaluation of anthropogenic secondary organic aerosol tracers from aromatic hydrocarbons, *Atmos. Chem. Phys.*, 17, 2053-2065, doi:10.5194/acp-17-2053-2017, 2017.
- Andreae, M. O., and Gelencser, A.: Black carbon or brown carbon? The nature of light-absorbing carbonaceous aerosols, *Atmos. Chem. Phys.*, 6, 3131-3148, doi:10.5194/acp-6-3131-2006, 2006.
- 495 Baduel, C., Monge, M. E., Voisin, D., Jaffrezzo, J., George, C., Haddad, I. E., Marchand, N., and Danna, B.: Oxidation of atmospheric humic like substances by ozone: a kinetic and structural analysis approach, *Environ. Sci. Technol.*, 45, 5238-5244, doi:10.1021/es200587z, 2011.



- Bertrand, A., Stefenelli, G., Jen, C. N., Pieber, S. M., Bruns, E. A., Ni, H., Temimeroussel, B., Slowik, J. G., Goldstein, A. H., Haddad, I. E., Baltensperger, U., Prevot, A. S. H., Wortham, H., and Marchand, N.: Evolution of the chemical fingerprint of biomass burning organic aerosol during aging, *Atmos. Chem. Phys.*, 18, 7607-7624, doi:10.5194/acp-18-7607-2018, 2018.
- Brege, M., Paglione, M., Gilardoni, S., Decesari, S., Facchini, M. C., and Mazzoleni, L.: Molecular insights on aging and aqueous-phase processing from ambient biomass burning emissions-influenced Po Valley fog and aerosol, *Atmos. Chem. Phys.*, 18, 13197-13214, doi:10.5194/acp-18-13197-2018, 2018.
- Chen, J., Qiu, S., Shang, J., Wilfrid, O. M., Liu, X., Tian, H., and Boman, J.: Impact of relative humidity and water soluble constituents of $PM_{2.5}$ on visibility impairment in Beijing, China, *Aerosol Air Qual. Res.*, 14, 260-268, doi:10.4209/aaqr.2012.12.0360, 2014.
- Chen, J., Li, C., Ristovski, Z., Milic, A., Gu, Y., Islam, M. S., Wang, S., Hao, J., Zhang, H., He, C., Guo, H., Fu, H., Miljevic, B., Morawska, L., Thai, P. K., Lam, Y. F., Pereira, G., Ding, A., Huang, X., and Dumka, U. C.: A review of biomass burning: Emissions and impacts on air quality, health and climate in China, *Sci. Total Environ.*, 579, 1000-1034, doi:10.1016/j.scitotenv.2016.11.025, 2017.
- Chen, P., Kang, K., Tripathi, L., Ram, K., Rupakheti, M., Panday, A. K., Zhang, Q., Guo, J., Wang, X., Pu, T., and Li, C.: Light absorption properties of elemental carbon (EC) and water-soluble brown carbon (WS-BrC) in the Kathmandu Valley, Nepal: a 5-year study, *Environ. Pollut.*, 261, 114239, doi:10.1016/j.envpol.2020.114239, 2020.
- Chen, Q., Wang, M., Wang, Y., Zhang, L., Li, Y., and Han, Y.: Oxidative potential of water-soluble matter associated with chromophoric substances in $PM_{2.5}$ over Xi'an, China, *Environ. Sci. Technol.*, 53, 8574-8584, doi:10.1021/acs.est.9b01976, 2019.
- Cheng, J., Su, J., Cui, T., Li, X., Dong, X., Sun, F., Yang, Y., Tong, D., Zheng, Y., Li, Y., Li, J., Zhang, Q., and He, K.: Dominant role of emission reduction in $PM_{2.5}$ air quality improvement in Beijing during 2013–2017: a model-based decomposition analysis, *Atmos. Chem. Phys.*, 19, 6125-6146, doi:10.5194/acp-19-6125-2019, 2019.
- Cheng, X., Li, H., Zhang, Y., Li, Y., Zhang, W., Wang, X., Bi, F., Zhang, H., Gao, J., Chai, F., Lun, X., Chen, Y., Gao, J., and Lu, J.: Atmospheric isoprene and monoterpenes in a typical urban area of Beijing: pollution characterization, chemical reactivity and source identification, *J. Environ. Sci.*, 71, 150-167, doi:10.1016/j.jes.2017.12.017, 2018.
- Cheng, Y., He, K., Duan, F., Zheng, M., Du, Z., Ma, Y., and Tan, J.: Ambient organic carbon to elemental carbon ratios: influences of the measurement methods and implications, *Atmos. Environ.*, 45, 2060-2066, doi:10.1016/j.atmosenv.2011.01.064, 2011.
- Cheng, Y., Engling, G., He, K., Duan, F., Ma, Y., Du, Z., Liu, J., Zheng, M., and Weber, R. J.: Biomass burning contribution to Beijing aerosol, *Atmos. Chem. Phys.*, 13, 7765-7781, doi:10.5194/acp-13-7765-2013, 2013.
- Cheng, Y., Zheng, G., Wei, C., Mu, Q., Zheng, B., Wang, Z., Gao, M., Zhang, Q., He, K., Carmichael, G. R., Poschl, U., and Su, H.: Reactive nitrogen chemistry in aerosol water as a source of sulfate during haze events in China, *Sci. Adv.*, 2, e1601530, doi:10.1126/sciadv.1601530, 2016.



- Claeys, M., Graham, B., Vas, G., Wang, W., Vermeylen, R., Pashynska, V., Cafmeyer, J., Guyon, P., Andreae, M. O., Artaxo, P., and Maenhaut, W.: Formation of secondary organic aerosols through photooxidation of isoprene, *Science*, 303, 1173-1176, doi:10.1126/science.1092805, 2004a.
- 535 Claeys, M., Wang, W., Ion, A. C., Kourtev, I., Gelencser, A., and Maenhaut, W.: Formation of secondary organic aerosols from isoprene and its gas-phase oxidation products through reaction with hydrogen peroxide, *Atmos. Environ.*, 38, 4093-4098, doi:10.1016/j.atmosenv.2004.06.001, 2004b.
- Ding, X., Zhang, Y., He, Q., Yu, Q., Wang, J., Shen, R., Song, W., Wang, Y., and Wang, X.: Significant increase of aromatics-derived secondary organic aerosol during fall to winter in China, *Environ. Sci. Technol.*, 51, 7432-7441, doi:10.1021/acs.est.6b06408, 2017.
- 540 Du, Z., He, K., Cheng, Y., Duan, F., Ma, Y., Liu, J., Zhang, X., Zheng, M., and Weber, R.: A yearlong study of water-soluble organic carbon in Beijing I: Sources and its primary vs. secondary nature, *Atmos. Environ.*, 92, 514-521, doi:10.1016/j.atmosenv.2014.04.060, 2014.
- Duan, F., He, K., Ma, Y., Ihozaki, T., Kawasaki, H., Arakawa, R., Kitayama, S., Tujimoto, K., Huang, T., Kimoto, T., Furutani, H., and Toyoda, M.: High molecular weight organic compounds (HMW-OCs) in severe winter haze: Direct observation and insights on the formation mechanism, *Environ. Pollut.*, 218, 289-296, doi:10.1016/j.envpol.2016.07.004, 2016.
- 545 Duan, J., Huang, R., Li, Y., Chen, Q., Zheng, Y., Chen, Y., Lin, C., Ni, H., Wang, M., Ovadnevaite, J., Ceburnis, D., Chen, C., Worsnop, D. R., Hoffmann, T., Odowd, C. D., and Cao, J.: Summertime and wintertime atmospheric processes of secondary aerosol in Beijing, *Atmos. Chem. Phys.*, 20, 3793-3807, doi:10.5194/acp-20-3793-2020, 2020.
- Elser, M., Huang, R. J., Wolf, R., Slowik, J. G., Wang, Q., Canonaco, F., Li, G., Bozzetti, C., Daellenbach, K. R., Huang, Y., Zhang, R., Li, Z., Cao, J., Baltensperger, U., El-Haddad, I., and Prevot, A. S. H.: New insights into PM_{2.5} chemical composition and sources in two major cities in China during extreme haze events using aerosol mass spectrometry, *Atmos. Chem. Phys.*, 16, 3207-3225, doi:10.5194/acp-16-3207-2016, 2016.
- 555 Ervens, B., Turpin, B. J., and Weber, R. J.: Secondary organic aerosol formation in cloud droplets and aqueous particles (aqSOA): a review of laboratory, field and model studies, *Atmos. Chem. Phys.*, 11, 11069-11102, doi:10.5194/acp-11-11069-2011, 2011.
- Fan, X., Wei, S., Zhu, M., Song, J., and Peng, P.: Comprehensive characterization of humic-like substances in smoke PM_{2.5} emitted from the combustion of biomass materials and fossil fuels, *Atmos. Chem. Phys.*, 6, 13321-13340, doi: 10.5194/acp-16-13321-2016, 2016.
- 560 Feng, B., Li, L., Xu, H., Wang, T., Wu, R., Chen, J., Zhang, Y., Liu, S., Ho, S. S. H., Cao, J., and Huang, W.: PM_{2.5}-bound polycyclic aromatic hydrocarbons (PAHs) in Beijing: seasonal variations, sources, and risk assessment, *J. Environ. Sci.*, 77, 11-19, doi:10.1016/j.jes.2017.12.025, 2018.



- Feng, T., Zhao, S., Bei, N., Wu, J., Liu, S., Li, X., Liu, L., Qian, Y., Yang, Q., Wang, Y., Zhou, W., Cao, J., and Li, G.:
565 Secondary organic aerosol enhanced by increasing atmospheric oxidizing capacity in Beijing–Tianjin–Hebei (BTH), China, *Atmos. Chem. Phys.*, 19, 7429–7443, doi:10.5194/acp-19-7429-2019, 2019.
- Fountoukis, C. and Nenes, A.: ISORROPIA II: a computationally efficient thermodynamic equilibrium model for K^+ - Ca^{2+} - Mg^{2+} - NH_4^+ - Na^+ - SO_4^{2-} - NO_3^- - Cl^- - H_2O aerosols, *Atmos. Chem. Phys.*, 7, 4639–4659, 2007.
- Frka, S., Grgic, I., Tursic, J., Gini, M. I., and Eleftheriadis, K.: Seasonal variability of carbon in humic-like matter of
570 ambient size-segregated water soluble organic aerosols from urban background environment, *Atmos. Environ.*, 173, 239–247, doi:10.1016/j.atmosenv.2017.11.013, 2018.
- Gaston, C. J., Lopezhilfiker, F. D., Whybrew, L. E., Hadley, O. L., McNair, F., Gao, H., Jaffe, D. A., and Thornton, J. A.: Online molecular characterization of fine particulate matter in Port Angeles, WA: evidence for a major impact from residential wood smoke, *Atmos. Environ.*, 138, 99–107, doi:10.1016/j.atmosenv.2016.05.013, 2016.
- 575 Geng, X., Mo, Y., Li, J., Zhong, C., Tang, J., Jiang, H., Ding, X., Malik, R. N., and Zhang, G.: Source apportionment of water-soluble brown carbon in aerosols over the northern South China Sea: Influence from land outflow, SOA formation and marine emission, *Atmos. Environ.*, 229, 117484, doi:10.1016/j.atmosenv.2020.117484, 2020.
- George, C., Ammann, M., Danna, B., Donaldson, D. J., and Nizkorodov, S. A.: Heterogeneous photochemistry in the atmosphere, *Chem. Rev.*, 115, 4218–4258, doi:10.1021/cr500648z, 2015.
- 580 Gilardoni, S., Massoli, P., Paglione, M., Giulianelli, L., Carbone, C., Rinaldi, M., Decesari, S., Sandrini, S., Costabile, F., Gobbi, G. P., Pietrogrande, M. C., Visentin, M., Scotto, F., Fuzzi, S., and Facchini, M. C.: Direct observation of aqueous secondary organic aerosol from biomass-burning emissions, *P. Natl. Sci. USA*, 113, 10013–10018, doi:10.1073/pnas.1602212113, 2016.
- Guo, S., Hu, M., Guo, Q., Zhang, X., Zheng, M., Zheng, J., Chang, C. C., Schauer, J. J., and Zhang, R.: Primary sources and
585 secondary formation of organic aerosols in Beijing, China, *Environ. Sci. Technol.*, 46, 9846–9853, doi:10.1021/es2042564, 2012.
- Guo, S., Hu, M., Zamora, M. L., Peng, J., Shang, D., Zheng, J., Du, Z., Wu, Z., Shao, M., Zeng, L., Molina, M. J., and Zhang, R.: Elucidating severe urban haze formation in China, *P. Natl. Sci. USA*, 2014, 111, 17373–17378, doi:10.1073/pnas.1419604111, 2014.
- 590 Hartikainen, A., Ylipirila, P., Tiitta, P., Leskinen, A., Kortelainen, M., Orasche, J., Schnellekreis, J., Lehtinen, K. E. J., Zimmermann, R., Jokiniemi, J., and Sippula, O.: Volatile organic compounds from logwood combustion: emissions and transformation under dark and photochemical aging conditions in a smog chamber, *Environ. Sci. Technol.*, 52, 4979–4988, doi:10.1021/acs.est.7b06269, 2018.
- Haynes, J. P., Miller, K. E., and Majestic, B. J.: Investigation into photoinduced auto-oxidation of polycyclic aromatic
595 hydrocarbons resulting in brown carbon production, *Environ. Sci. Technol.*, 53, 682–691, doi:10.1021/acs.est.8b05704, 2019.
- Hennigan, C. J., Bergin, M. H., Russell, A. G., Nenes, A., and Weber, R. J.: Gas/particle partitioning of water-soluble organic aerosol in Atlanta, *Atmos. Chem. Phys.*, 9, 3613–3628, doi:10.5194/acp-9-3613-2009, 2009.



- Hu, W., Hu, M., Hu, W., Jimenez, J. L., Yuan, B., Chen, W., Wang, M., Wu, Y., Chen, C., Wang, Z., Peng, J., Zeng, L., and Shao, M.: Chemical composition, sources, and aging process of submicron aerosols in Beijing: Contrast between summer and winter, *J. Geophys. Res. Atmos.*, 121, 1955-1977, doi:10.1002/2015JD024020, 2016.
- Hu, W., Hu, M., Hu, W., Zheng, J., Chen, C., Wu, Y., and Guo, S.: Seasonal variations in high time-resolved chemical compositions, sources, and evolution of atmospheric submicron aerosols in the megacity Beijing, *Atmos. Chem. Phys.*, 17, 9979-10000, doi:10.5194/acp-17-9979-2017, 2017.
- Huang, G., Liu, Y., Shao, M., Li, Y., Chen, Q., Zheng, Y., Wu, Z., Liu, Y., Wu, Y., Hu, M., Li, X., Lu, S., Wang, C., Liu, J., Zheng, M., and Zhu, T.: Potentially important contribution of gas-phase oxidation of naphthalene and methylnaphthalene to secondary organic aerosol during haze events in Beijing, *Environ. Sci. Technol.*, 53, 1235-1244, doi:10.1021/acs.est.8b04523, 2019.
- Huang, R. J., Zhang, Y., Bozzetti, C., Ho, K., Cao, J., Han, Y., Daellenbach, K. R., Slowik, J. G., Platt, S. M., Canonaco, F., Zotter, P., Wolf, R., Pieber, S. M., Bruns, E. A., Crippa, M., Ciarelli, G., Piazzalunga, A., Schwikowski, M., Abbaszade, G., Schnellekreis, J., Zimmermann, R., An, Z., Szidat, S., Baltensperger, U., Haddad, I. E., and Prevot, A. S. H.: High secondary aerosol contribution to particulate pollution during haze events in China, *Nature*, 2014, 514, 218-222, doi:10.1038/nature13774, 2014.
- Huang, R. J., Yang, L., Shen, J., Yuan, W., Gong, Y., Guo, J., Cao, W., Duan, J., Ni, H., Zhu, C., Dai, W., Li, Y., Chen, Y., Chen, Q., Wu, Y., Zhang, R., Dusek, U., O'Dowd, C., and Hoffmann, T.: Water-insoluble organics dominate brown carbon in wintertime urban aerosol of China: chemical characteristics and optical properties, *Environ. Sci. Technol.*, doi:10.1021/acs.est.0c01149, 2020.
- Iinuma, Y., Boge, O., Grafe, R., and Herrmann, H.: Methyl-nitrocatechols: atmospheric tracer compounds for biomass burning secondary organic aerosols, *Environ. Sci. Technol.*, 44, 8453-8459, doi:10.1021/es102938a, 2010.
- Islam, M. R., Jayarathne, T., Simpson, I. J., Werden, B., Maben, J. R., Gilbert, A., Praveen, P. S., Adhikari, S., Panday, A. K., Rupakheti, M., Blake, D. R., Yokelson, R. J., Decarlo, P. F., Keene, W. C., and Stone, E. A.: Ambient air quality in the Kathmandu Valley, Nepal, during the pre-monsoon: concentrations and sources of particulate matter and trace gases, *Atmos. Chem. Phys.*, 20, 2927-2951, doi:10.5194/acp-20-2927-2020, 2020.
- Ji, Y., Shi, Q., Li, Y., An, T., Zheng, J., Peng, J., Gao, Y., Chen, J., Li, G., Wang, Y., Zhang, F., Zhang, A. L., Zhao, J., Molina, M. J., and Zhang, R.: Carbenium ion-mediated oligomerization of methylglyoxal for secondary organic aerosol formation, *P. Natl. Sci. USA*, doi:10.1073/pnas.1912235117, 2020.
- Jia, L., and Xu, Y.: Different roles of water in secondary organic aerosol formation from toluene and isoprene, *Atmos. Chem. Phys.*, 18, 8137-8154, doi:10.5194/acp-18-8137-2018, 2018.
- Jimenez, J. L., Canagaratna, M. R., Donahue, N. M., Prevot, A. S. H., Zhang, Q., Kroll, J. H., Decarlo, P. F., Allan, J. D., Coe, H., Ng, N. L., Aiken, A. C., Docherty, K. S., Ulbrich, I. M., Grieshop, A. P., Robinson, A. L., Duplissy, J., Smith, J. D., Wilson, K. R., Lanz, V. A., Hueglin, C., Sun, Y., Tian, J., Laaksonen, A., Raatikainen, T., Rautiainen, J., Vaattovaara, P., Ehn, M., Kulmala, M., Tomlinson, J., Collins, D. R., Cubison, M. J., Dunlea, E. J., Huffman, J. A., Onasch, T. B., Alfarra, M.



- R., Williams, P. I., Bower, K. N., Kondo, Y., Schneider, J., Drewnick, J., Borrmann, S., Weimer, S., Demerjian, K. L., Salcedo, D., Cottrell, L., Griffin, R. J., Takami, A., Miyoshi, T., Hatakeyama, S., Shimono, A., Sun, J., Zhang, Y., Dzepina, K., Kimmel, J. R., Sueper, D., Jayne, J. T., Herndon, S. C., Trimborn, A., Williams, L. R., Wood, E. C., Middlebrook, A. M., Kolb, C. E., Baltensperger, U., and Worsnop, D. R.: Evolution of organic aerosols in the atmosphere, *Science*, 326, 1525-1529, doi:10.1126/science.1180353, 2009.
- Kahnt, A., Behrouzi, S., Vermeylen, R., Shalamzari, M. S., Vercauteren, J., Roekens, E., Claeys, M., and Maenhaut, W.: One-year study of nitro-organic compounds and their relation to wood burning in PM₁₀ aerosol from a rural site in Belgium, *Atmos. Environ.*, 81, 561-568, doi:10.1016/j.atmosenv.2013.09.041, 2013.
- Kamens, R. M., Zhang, H., Chen, E. H., Zhou, Y., Parikh, H. M., Wilson, R. L., Galloway, K. E., and Rosen, E. P.: Secondary organic aerosol formation from toluene in an atmospheric hydrocarbon mixture: Water and particle seed effects, *Atmos. Environ.*, 45, 2324-2334, doi:10.1016/j.atmosenv.2010.11.007, 2011.
- Kang, M., Fu, P., Kawamura, K., Yang, F., Zhang, H., Zang, Z., Ren, H., Ren, L., Zhao, Y., Sun, Y., and Wang, Z.: Characterization of biogenic primary and secondary organic aerosols in the marine atmosphere over the East China Sea, *Atmos. Chem. Phys.*, 18, 13947-13967, doi:10.5194/acp-18-13947-2018, 2018a.
- Kang, M., Ren, L., Ren, H., Zhao, Y., Kawamura, K., Zhang, H., Wei, L., Sun, Y., Wang, Z., and Fu, P.: Primary biogenic and anthropogenic sources of organic aerosols in Beijing, China: Insights from saccharides and n-alkanes, *Environ. Pollut.*, 243, 1579-1587, doi:10.1016/j.envpol.2018.09.118, 2018b.
- Kaur, R., Labins, J. R., Helbock, S. S., Jiang, W., Bein, K. J., Zhang, Q., and Anastasio, C.: Photooxidants from brown carbon and other chromophores in illuminated particle extracts, *Atmos. Chem. Phys.*, 19, 6579-6594, doi:10.5194/acp-19-6579-2019, 2019.
- Kawamura, K., and Yasui, O.: Diurnal changes in the distribution of dicarboxylic acids, ketocarboxylic acids and dicarbonyls in the urban Tokyo atmosphere, *Atmos. Environ.*, 39, 1945-1960, doi:10.1016/j.atmosenv.2004.12.014, 2005.
- Kourtchev, I., Copolovici, L., Claeys, M., and Maenhaut, W.: Characterization of atmospheric aerosols at a forested site in Central Europe, *Environ. Sci. Technol.*, 43, 4665-4671, doi:10.1021/es803055w, 2009.
- Kuang, Y., He, Y., Xu, W., Zhao, P., Cheng, Y., Zhao, G., Tao, J., Ma, N., Su, H., Zhang, Y., Sun, J., Cheng, P., Yang, W., Zhang, S., Wu, C., Sun, Y., and Zhao, C.: Distinct diurnal variation in organic aerosol hygroscopicity and its relationship with oxygenated organic aerosol, *Atmos. Chem. Phys.*, 20, 865-880, doi:10.5194/acp-20-865-2020, 2020.
- Larsen, B. R., Bella, D. D., Glasius, M., Winterhalter, R., Jensen, N. R., and Hjorth, J.: Gas-phase OH oxidation of monoterpenes: gaseous and particulate products, *J. Atmos. Chem.*, 38, 231-276, doi:10.1023/A:1006487530903, 2001.
- Li, H., Zhang, Q., Zhang, Q., Chen, C., Wang, L., Wei, Z., Zhou, S., Parworth, C. L., Zheng, B., Canonaco, F., Prevot, A. S. H., Chen, P., Zhang, H., Wallington, T. J., and He, K.: Wintertime aerosol chemistry and haze evolution in an extremely polluted city of the North China Plain: significant contribution from coal and biomass combustion, *Atmos. Chem. Phys.*, 17, 4751-4768, doi:10.5194/acp-17-4751-2017, 2017.



- 665 Li, J., Wang, G., Cao, J., Wang, X., and Zhang, R.: Observation of biogenic secondary organic aerosols in the atmosphere of
 a mountain site in central China: temperature and relative humidity effects, *Atmos. Chem. Phys.*, 13, 11535-11549,
 doi:10.5194/acp-13-11535-2013, 2013
- Li, J., Du, H., Wang, Z., Sun, Y., Yang, W., Li, J., Tang, X., and Fu, P.: Rapid formation of a severe regional winter haze
 episode over a mega-city cluster on the North China Plain, *Environ. Pollut.*, 223, 605-615, doi:10.1016/j.envpol.2017.01.063,
 670 2017.
- Li, J., Wang, G., Wu, C., Cao, C., Ren, Y., Wang, J., Li, J., Cao, J., Zeng, L., and Zhu, T.: Characterization of isoprene-
 derived secondary organic aerosols at a rural site in North China Plain with implications for anthropogenic pollution effects,
Sci. Rep., 8, 535, doi:10.1038/s41598-017-18983-7, 2018.
- Li, L., Ren, L., Ren, H., Yue, S., Xie, Q., Zhao, W., Kang, M., Li, J., Wang, Z., Sun, Y., and Fu, P.: Molecular
 675 characterization and seasonal variation in primary and secondary organic aerosols in Beijing, China, *J. Geophys. Res.*
Atmos., 123, 12394-12412, doi:10.1029/2018JD028527, 2018.
- Li, X., Han, J., Hopke, P. K., Hu, J., Shu, Q., Chang, Q., and Ying, Q.: Quantifying primary and secondary humic-like
 substances in urban aerosol based on emission source characterization and a source-oriented air quality model, *Atmos. Chem.*
Phys., 19, 2327-2341, doi:10.5194/acp-19-2327-2019, 2019a
- 680 Li, X., Wu, J., Elser, M., Tong, S., Liu, S., Li, X., Liu, L., Cao, J., Zhou, J., Elhaddad, I., Huang, R., Ge, M., Tie, X., Prevot,
 A. S. H., and Li, G.: Wintertime secondary organic aerosol formation in Beijing-Tianjin-Hebei (BTH): contributions of
 HONO sources and heterogeneous reactions, *Atmos. Chem. Phys.*, 19, 2343-2359, doi:10.5194/acp-19-2343-2019, 2019b.
- Li, X., Yang, K., Han, J., Ying, Q., and Hopke, P. K.: Sources of humic-like substances (HULIS) in PM_{2.5} in Beijing:
 receptor modeling approach, *Sci. Total Environ.*, 671, 765-775, doi:10.1016/j.scitotenv.2019.03.333, 2019c.
- 685 Li, Y., Huang, D., Cheung, H. Y., Lee, A. K. Y., and Chan, C. K.: Aqueous-phase photochemical oxidation and direct
 photolysis of vanillin - a model compound of methoxy phenols from biomass burning, *Atmos. Chem. Phys.*, 14, 27641-
 27675, doi:10.5194/acp-14-2871-2014, 2014.
- Liang, L., Engling, G., Duan, F., Cheng, Y., and He, K.: Characteristics of 2-methyltetrols in ambient aerosol in Beijing,
 China, *Atmos. Environ.*, 59, 376-381, doi:10.1016/j.atmosenv.2012.05.052, 2012.
- 690 Liggio, J., and Li, S.: Reactive uptake of pinonaldehyde on acidic aerosols, *J. Geophys. Res. Atmos.*, 111, D24303,
 doi:10.1029/2005JD006978, 2006.
- Liu, J., Mauzerall, D. L., Chen, Q., Zhang, Q., Song, Y., Peng, W., Klimont, Z., Qiu, X., Zhang, S., Hu, M., Lin, W., Smith,
 K. R., and Zhu, T.: Air pollutant emissions from Chinese households: a major and underappreciated ambient pollution source,
P. Natl. Sci. USA, 113, 7756-7761, doi:10.1073/pnas.1604537113, 2016.
- 695 Lu, J., Ge, X., Liu, Y., Chen, Y., Xie, X., Ou, Y., Ye, Z., and Chen, M.: Significant secondary organic aerosol production
 from aqueous-phase processing of two intermediate volatility organic compounds, *Atmos. Environ.*, 211, 63-68,
 doi:10.1016/j.atmosenv.2019.05.014, 2019.



- Ma, Y., Cheng, Y., Qiu, X., Gao, G., Fang, Y., Wang, J., Zhu, T., Yu, J. Z., and Hu, D.: Sources and oxidative potential of water-soluble humic-like substances (HULIS_{WS}) in fine particulate matter (PM_{2.5}) in Beijing, *Atmos. Chem. Phys.*, 18, 5607-5617, doi:10.5194/acp-18-5607-2018, 2018.
- Ma, T., Furutani, H., Duan, F., Kimoto, T., Jiang, J., Zhang, Q., Xu, X., Wang, Y., Gao, J., Geng, G., Li, M., Song, S., Ma, Y., Che, F., Wang, J., Zhu, L., Huang, T., Toyoda, M., and He, K.: Contribution of hydroxymethanesulfonate (HMS) to severe winter haze in the North China Plain, *Atmos. Chem. Phys.*, 1-17, doi:10.5194/acp-2020-113, 2020.
- Manfrin, A., Nizkorodov, S. A., Malecha, K. T., Getzinger, G. J., McNeill, K., and Borduasdedekind, N.: Reactive oxygen species production from secondary organic aerosols: the importance of singlet oxygen, *Environ. Sci. Technol.*, 53, 8553-8562, doi: 10.1021/acs.est.9b01609, 2019.
- Miyazaki, Y., Kondo, Y., Shiraiwa, M., Takegawa, N., Miyakawa, T., Han, S., Kita, K., Hu, M., Deng, Z., Zhao, Y., Sugimoto, N., Blake, D. R., Weber, R. J.: Chemical characterization of water-soluble organic carbon aerosols at a rural site in the Pearl River Delta, China, in the summer of 2006, *J. Geophys. Res. Atmos.*, 114, D12408, doi:doi:10.1029/2009JD011736, 2009.
- Pang, H., Zhang, Q., Lu, X., Li, K., Chen, H., Chen, J., Yang, X., Ma, Y., Ma, J., and Cheng, H.: Nitrite-mediated photooxidation of vanillin in the atmospheric aqueous phase, *Environ. Sci. Technol.*, 53, 14253-14263, doi:10.1021/acs.est.9b03649, 2020.
- Qian, X., Shen, H., and Chen, Z.: Characterizing summer and winter carbonyl compounds in Beijing atmosphere, *Atmos. Environ.*, 214, 116845, doi:10.1016/j.atmosenv.2019.116845, 2019.
- Qiu, Y., Xu, W., Jia, L., He, Y., Fu, P., Zhang, Q., Xie, Q., Hou, S., Xie, C., Xu, Y., Wang, Z., Worsnop, D. R., and Sun, Y.: Molecular composition and sources of water-soluble organic aerosol in summer in Beijing, *Chemosphere*, 225, 126850, doi:10.1016/j.chemosphere.2020.126850, 2020.
- Qu, Y., Chen, Y., Liu, X., Zhang, J., Guo, Y., and An, J.: Seasonal effects of additional HONO sources and the heterogeneous reactions of N₂O₅ on nitrate in the North China Plain, *Sci. Total Environ.*, 690, 97-107, doi:10.1016/j.scitotenv.2019.06.436, 2019.
- Shen, R., Ding, X., He, Q., Cong, Z., Yu, Q., and Wang, X.: Seasonal variation of secondary organic aerosol tracers in Central Tibetan Plateau, *Atmos. Chem. Phys.*, 15, 8781-8793, doi:10.5194/acp-15-8781-2015, 2015.
- Shen, X., Vogel, H., Vogel, B., Huang, W., Mohr, C., Ramisetty, R., Leisner, T., Prevot, A. S. H., and Saathoff, H.: Composition and origin of PM_{2.5} aerosol particles in the upper Rhine valley in summer, *Atmos. Chem. Phys.*, 19, 13189-13208, doi:10.5194/acp-19-13189-2019, 2019.
- Smith, J. D., Kinney, H., and Anastasio, C.: Phenolic carbonyls undergo rapid aqueous photodegradation to form low-volatility, light-absorbing products, *Atmos. Environ.*, 126, 36-44, doi:10.1016/j.atmosenv.2015.11.035, 2016.
- Sun, J., Wu, F., Hu, B., Tang, G., Zhang, J., and Wang, Y.: VOC characteristics, emissions and contributions to SOA formation during hazy episodes, *Atmos. Environ.*, 2016, 141, 560-570, doi:10.1016/j.atmosenv.2016.06.060, 2016.



- Sun, Y., Zhang, Q., Anastasio, C., and Sun, J.: Insights into secondary organic aerosol formed via aqueous-phase reactions of phenolic compounds based on high resolution mass spectrometry, *Atmos. Chem. Phys.*, 10, 4809-4822, doi:10.5194/acp-10-4809-2010, 2010.
- 735 Sun, Y., Xu, W., Zhang, Q., Jiang, Q., Canonaco, F., Prevot, A. S. H., Fu, P., Li, J., Jayne, J. T., Worsnop, D. R., and Wang, Z.: Source apportionment of organic aerosol from 2-year highly time-resolved measurements by an aerosol chemical speciation monitor in Beijing, China, *Atmos. Chem. Phys.*, 18, 8469-8489, doi:10.5194/acp-18-8469-2018, 2018.
- Surratt, J. D., Chan, A. W., Eddingsaas, N. C., Chan, M., Loza, C. L., Kwan, A. J., Hersey, S. P., Flagan, R. C., Wennberg, P. O., and Seinfeld, J. H.: Reactive intermediates revealed in secondary organic aerosol formation from isoprene, *P. Natl. Sci. USA*, 107, 6640-6645, doi:10.1073/pnas.091114107, 2010.
- 740 Tang, R., Wu, Z., Li, X., Wang, Y., Shang, D., Xiao, Y., Li, M., Zeng, L., Wu, Z., Hallquist, M., Hu, M., and Guo, S.: Primary and secondary organic aerosols in summer 2016 in Beijing, *Atmos. Chem. Phys.*, 18, 4055-4068, doi:10.5194/acp-18-4055-2018, 2018.
- Tang, X., Zhang, X., Wang, Z., and Ci, Z.: Water-soluble organic carbon (WSOC) and its temperature-resolved carbon fractions in atmospheric aerosols in Beijing, *Atmos. Res.*, 181, 200-210, doi:10.1016/j.atmosres.2016.06.019, 2016.
- 745 Tao, J., Zhang, L., Zhang, R., Wu, Y., Zhang, Z., Zhang, X., Tang, Y., Cao, J., and Zhang, Y.: Uncertainty assessment of source attribution of PM_{2.5} and its water-soluble organic carbon content using different biomass burning tracers in positive matrix factorization analysis-a case study in Beijing, China, *Sci. Total Environ.*, 543, 326-335, doi:10.1016/j.scitotenv.2015.11.057, 2016.
- van Drooge, B. L., Fontal, M., Fernández, P., Fernández, M. A., Muñoz-Arnanz, J., Jiménez, B., and Grimalt, J. O.: Organic molecular tracers in atmospheric PM₁ at urban intensive traffic and background sites in two high-insolation European cities, *Atmos. Environ.*, 188, 71-81, doi:10.1016/j.atmosenv.2018.06.024, 2018.
- Verma, V., Ricomartinez, R., Kotra, N., King, L. E., Liu, J., Snell, T. W., and Weber, R. J.: Contribution of water-soluble and insoluble components and their hydrophobic/hydrophilic subfractions to the reactive oxygen species-generating potential of fine ambient aerosols, *Environ. Sci. Technol.*, 46, 11384-11392, doi:10.1021/es302484r, 2012.
- 755 Verma, V., Fang, T., Xu, L., Peltier, R. E., Russell, A. G., Ng, N. L., and Weber, R. G.: Organic aerosols associated with the generation of reactive oxygen species (ROS) by water-soluble PM_{2.5}, *Environ. Sci. Technol.*, 49, 4646-4656, doi:10.1021/es505577w, 2015.
- Vidovic, K., Jurkovic, D. L., Sala, M., Kroflic, A., and Grgic, I.: Nighttime aqueous-phase formation of nitrocatechols in the atmospheric condensed phase, *Environ. Sci. Technol.*, 52, 9722-9730, doi:10.1021/acs.est.8b01161, 2018.
- 760 Vione, D., Albinet, A., Barsotti, F., Mekic, M., Jiang, B., Minero, C., Brigante, M., and Gligorovski, S.: Formation of substances with humic-like fluorescence properties, upon photoinduced oligomerization of typical phenolic compounds emitted by biomass burning, *Atmos. Environ.*, 206, 197-207, doi:10.1016/j.atmosenv.2019.03.005, 2019.



- Wang, Y., Zhang, X., and Draxler, R. R.: TrajStat: GIS-based software that uses various trajectory statistical analysis methods to identify potential sources from long-term air pollution measurement data, *Environ. Modell. Softw.*, 24, 938-939, doi:10.1016/j.envsoft.2009.01.004, 2009.
- Wang, Y., Hu, M., Wang, Y., Zheng, J., Shang, D., Yang, Y., Liu, Y., Li, X., Tang, R., Zhu, W., Du, Z., Wu, Y., Guo, S., Wu, Z., Lou, S., Hallquist, M., and Yu, J.: The formation of nitro-aromatic compounds under high NO_x and anthropogenic VOC conditions in urban Beijing, China, *Atmos. Chem. Phys.*, 19, 7649-7665.
- Wang, Y., Wang, M., Li, S., Sun, H., Mu, Z., Zhang, L., Li, Y., and Chen, Q.: Study on the oxidation potential of the water-soluble components of ambient PM_{2.5} over Xi'an, China: pollution levels, source apportionment and transport pathways, *Environ. Int.*, 136, 105515, doi:10.1016/j.envint.2020.105515, 2020.
- Wiedinmyer, C., Akagi, S. K., Yokelson, R. J., Emmons, L. K., Al-Saadi, J. A., Orlando, J. J., and Soja, A. J.: The Fire INventory from NCAR (FINN): a high resolution global model to estimate the emissions from open burning, *Geosci. Model. Dev.*, 4, 625-641, doi:10.5194/gmd-4-625-2011, 2011.
- Wu, J., Bei, N., Hu, B., Liu, S., Zhou, M., Wang, Q., Li, X., Liu, L., Feng, T., Liu, Z., Wang, Y., Cao, J., Tie, X., Wang, J., Molina, L. T., and Liu, G.: Is water vapor a key player of the wintertime haze in North China Plain, *Atmos. Chem. Phys.*, 19, 8721-8739, doi:10.5194/acp-19-8721-2019, 2019.
- Wu, Z., Zheng, J., Shang, D., Du, Z., Wu, Y., Zeng, L., Wiedensohler, A., and Hu, M.: Particle hygroscopicity and its link to chemical composition in the urban atmosphere of Beijing, China, during summertime, *Atmos. Chem. Phys.*, 16, 1123-1138, doi:10.5194/acp-16-1123-2016, 2016.
- Xu, L., Guo, H., Boyd, C. M., Klein, M., Bougiatioti, A., Cerully, K. M., Hite, J. R., Isaacman-VanWertz, G., Kreisberg, N. M., Knote, C., Olson, K., Koss, A., Goldstein, A. H., Hering, S. V., de Gouw, J., Baumann, K., Lee, S. H., Nenes, A., Weber, R. J., and Ng, N. L.: Effects of anthropogenic emissions on aerosol formation from isoprene and monoterpenes in the southeastern United States, *P. Natl. Sci. USA*, 112, 37-42, doi:10.1073/pnas.1417609112, 2015.
- Xu, S., Ren, L., Lang, Y., Hou, S., Ren, H., Wei, L., Wu, L., Deng, J., Hu, W., Pan, X., Sun, Y., Wang, Z., Su, H., Cheng, Y., and Fu, P.: Molecular markers of biomass burning and primary biological aerosols in urban Beijing: size distribution and seasonal variation, *Atmos. Chem. Phys.*, doi:10.5194/acp-2019-841, 2020.
- Xu, W., Han, T., Du, W., Wang, Q., Chen, C., Zhao, J., Zhang, Y., Li, J., Fu, P., Wang, Z., Worsnop, D. R., and Sun, Y.: Effects of aqueous-phase and photochemical processing on secondary organic aerosol formation and evolution in Beijing, China, *Environ. Sci. Technol.*, 51, 762-770, doi:10.1021/acs.est.6b04498, 2017.
- Yan, C., Zheng, M., Sullivan, A. P., Bosch, C., Desyaterik, Y., Andersson, A., Li, X., Guo, X., Zhou, T., Gustafsson, O., and Collett, J. L.: Chemical characteristics and light-absorbing property of water-soluble organic carbon in Beijing: Biomass burning contributions, *Atmos. Environ.*, 121, 4-12, doi:10.1016/j.atmosenv.2015.05.005, 2015.
- Yan, C., Zheng, M., Sullivan, A. P., Shen, G., Chen, Y., Wang, S., Zhao, B., Cai, S., Desyaterik, Y., Li, X., Zhou, T., Gustafsson, O., and Collett, J. L.: Residential coal combustion as a source of levoglucosan in China, *Environ. Sci. Technol.*, 52, 1665-1674, doi:10.1021/acs.est.7b05858, 2018.



- Yan, C., Sullivan, A. P., Cheng, Y., Zheng, M., Zhang, Y., Zhu, T., and Collett, J. L.: Characterization of saccharides and associated usage in determining biogenic and biomass burning aerosols in atmospheric fine particulate matter in the North China Plain, *Sci. Total Environ.*, 650, 2939-2950, doi:10.1016/j.scitotenv.2018.09.325, 2019.
- 800 Yang, H., Chen, J., Wen, J., Tian, H., and Liu, X.: Composition and sources of PM_{2.5} around the heating periods of 2013 and 2014 in Beijing: implications for efficient mitigation measures, *Atmos. Environ.*, 124, 378-386, doi:10.1016/j.atmosenv.2015.05.015, 2016.
- Yang, S., Duan, F., Ma, Y., He, K., Zhu, L., Ma, T., Ye, S., Li, H., Huang, T., and Kimoto, T.: Haze formation indicator based on observation of critical carbonaceous species in the atmosphere, *Environ. Pollut.*, 244, 84-92, 805 doi:10.1016/j.envpol.2018.10.006, 2019.
- Yu, H., Wei, J., Cheng, Y., Subedi, K., and Verma, V.: Synergistic and antagonistic interactions among the particulate matter components in generating reactive oxygen species based on the dithiothreitol assay, *Environ. Sci. Technol.*, 52, 2261-2270, doi:10.1021/acs.est.7b04261, 2018.
- Yu, J. Z., Cocker, D. R., Griffin, R. J., Flagan, R. C., and Seinfeld, J. H.: Gas-phase ozone oxidation of monoterpenes: 810 Gaseous and particulate products, *J. Atmos. Chem.*, 34, 207-258, doi:10.1023/A:1006487530903, 1999.
- Yu, L., Smith, J., Laskin, A., Anastasio, C., Laskin, J., and Zhang, Q.: Chemical characterization of SOA formed from aqueous-phase reactions of phenols with the triplet excited state of carbonyl and hydroxyl radical, *Atmos. Chem. Phys.*, 14, 13801-13816, doi:10.5194/acp-14-13801-2014, 2014.
- Yu, Q., Chen, J., Qin, W., Cheng, S., Zhang, Y., Ahmad, M., and Ouyang, W.: Characteristics and secondary formation of 815 water-soluble organic acids in PM₁, PM_{2.5} and PM₁₀ in Beijing during haze episodes, *Sci. Total Environ.*, 669, 175-184, doi:10.1016/j.scitotenv.2019.03.131, 2019.
- Zhang, C., Zou, Z., Chang, Y., Zhang, Y., Wang, X., and Yang, X.: Source assessment of atmospheric fine particulate matter in a Chinese megacity: insights from long-term, high-time resolution chemical composition measurements from Shanghai flagship monitoring supersite, *Chemosphere*, 251, 126598, doi:10.1016/j.chemosphere.2020.126598, 2020.
- 820 Zhang, J., Sun, Y., Liu, Z., Ji, D., Hu, B., Liu, Q., and Wang, Y.: Characterization of submicron aerosols during a month of serious pollution in Beijing, 2013, *Atmos. Chem. Phys.*, 14, 2887-2903, doi:10.5194/acp-14-2887-2014, 2014.
- Zhang, R., Khalizov, A., Wang, L., Hu, M., and Xu, W.: Nucleation and growth of nanoparticles in the atmosphere, *Chem. Rev.*, 112, 1957-2011, doi:10.1021/cr2001756, 2012.
- Zhang, Y., Shao, M., Zhang, Y., Zeng, L., He, L., Zhu, B., Wei, J., and Zhu, X.: Source profiles of particulate organic 825 matters emitted from cereal straw burnings, *J. Environ. Sci.*, 19, 167-175, doi:10.1016/S1001-0742(07)60027-8, 2007.
- Zhang, Y., El-Haddad, I., Huang, R., Ho, K., Cao, J., Han, Y., Zotter, P., Bozzetti, C., Daellenbach, K. R., Slowik, J. G., Salazar, G., Prevot, A. S. H., and Szidat, S.: Large contribution of fossil fuel derived secondary organic carbon to water soluble organic aerosols in winter haze in China, *Atmos. Chem. Phys.*, 18, 4005-4017, doi:10.5194/acp-18-4005-2018, 2018.
- Zhao, W., Kawamura, K., Yue, S., Wei, L., Ren, H., Yan, Y., Kang, M., Li, L., Ren, L., Lai, S., Li, J., Sun, Y., Wang, Z., 830 and Fu, P.: Molecular distribution and compound-specific stable carbon isotopic composition of dicarboxylic acids,



- oxocarboxylic acids and α -dicarbonyls in PM_{2.5} from Beijing, China, *Atmos. Chem. Phys.*, 18, 2749-2767, doi:10.5194/acp-18-2749-2018, 2018.
- Zhao, Y., Hu, M., Slanina, S., and Zhang, Y.: Chemical compositions of fine particulate organic matter emitted from Chinese cooking, *Environ. Sci. Technol.*, 41, 99-105, doi:10.1021/es0614518, 2007.
- 835 Zhao, Y., Kreisberg, N. M., Worton, D. R., Isaacman, G., Weber, R., Liu, S., Day, D. A., Russell, L. M., Markovic, M. Z., Vandenboer, T. C., Murphy, J. G., Hering, S. V., and Goldstein, A. H.: Insights into secondary organic aerosol formation mechanisms from measured gas/particle partitioning of specific organic tracer compounds, *Environ. Sci. Technol.*, 47, 3781-3787, doi:10.1021/es304587x, 2013.
- 840 Zhou, C., Jang, M., and Yu, Z.: Simulation of SOA formation from the photooxidation of monoalkylbenzenes in the presence of aqueous aerosols containing electrolytes under various NO_x levels, *Atmos. Chem. Phys.*, 19, 5719-5735, doi:10.5194/acp-19-5719-2019, 2019.



Table 1 The mean concentrations of the identified carbonaceous species in PM_{2.5} over the sampling periods in four seasons.

| Compounds | Winter | | | Spring | | | Summer | | | Autumn | | |
|--------------------------------------------|--------|-------|-------|--------|-------|-------|--------|-------|------|--------|-------|-------|
| | Day | Night | Mean | Day | Night | Mean | Day | Night | Mean | Day | Night | Mean |
| PM _{2.5} (µg m ⁻³) | 119.6 | 147.1 | 133.3 | 60.6 | 64.5 | 62.5 | 59.8 | 51.9 | 55.8 | 75.2 | 81.1 | 78.2 |
| OC (µg m ⁻³) | 20.1 | 21.0 | 20.6 | 7.9 | 9.5 | 8.7 | 8.7 | 6.8 | 7.8 | 9.4 | 10.1 | 9.7 |
| EC (µg m ⁻³) | 3.9 | 4.7 | 4.3 | 1.9 | 2.7 | 2.3 | 1.4 | 1.3 | 1.3 | 2.4 | 3.4 | 2.9 |
| OC/EC | 4.64 | 4.27 | 4.45 | 5.13 | 4.36 | 4.75 | 6.74 | 5.32 | 6.06 | 4.40 | 3.26 | 3.83 |
| WSOC (µg m ⁻³) | 11.4 | 12.0 | 11.7 | 4.1 | 4.7 | 4.4 | 5.3 | 4.0 | 4.7 | 4.7 | 4.9 | 4.8 |
| WSOC/OC | 0.53 | 0.51 | 0.52 | 0.50 | 0.47 | 0.49 | 0.62 | 0.59 | 0.60 | 0.47 | 0.46 | 0.46 |
| Hydrophobic WSOC (µg m ⁻³) | 7.9 | 8.0 | 8.0 | 2.8 | 2.9 | 2.9 | 4.1 | 3.4 | 3.8 | 2.9 | 2.9 | 2.9 |
| Hydrophilic WSOC (µg m ⁻³) | 3.2 | 4.0 | 3.6 | 1.3 | 1.8 | 1.6 | 1.2 | 0.7 | 1.0 | 1.8 | 2.0 | 1.9 |
| Organic tracers (ng m⁻³) | | | | | | | | | | | | |
| Levogluconan | 306.9 | 387.8 | 348.8 | 100.0 | 194.1 | 147.1 | 23.6 | 34.2 | 28.9 | 135.8 | 233.8 | 184.8 |
| Cholesterol | 5.0 | 4.9 | 4.9 | 3.9 | 4.8 | 4.3 | 4.1 | 3.0 | 3.6 | 6.1 | 6.3 | 6.2 |
| Phthalic acid | 88.7 | 90.8 | 89.8 | 27.3 | 21.9 | 24.6 | 55.9 | 17.6 | 36.8 | 27.6 | 19.9 | 23.8 |
| 4-Methyl-5-nitrocatechol | 24.7 | 35.2 | 30.1 | 1.8 | 3.3 | 2.6 | 0.1 | 0.0 | 0.1 | 1.6 | 4.4 | 3.0 |
| 2-Methylerythritol | 2.1 | 2.2 | 2.2 | 1.2 | 1.5 | 1.4 | 55.4 | 41.6 | 48.5 | 2.3 | 2.6 | 2.5 |
| 3-Hydroxyglutaric acid | 4.4 | 4.2 | 4.3 | 4.2 | 4.9 | 4.6 | 37.1 | 27.3 | 32.2 | 7.5 | 7.0 | 7.2 |
| cis-Pinonic acid | 3.3 | 3.0 | 3.2 | 9.0 | 6.9 | 7.9 | 7.3 | 10.1 | 8.7 | 7.3 | 3.6 | 5.5 |

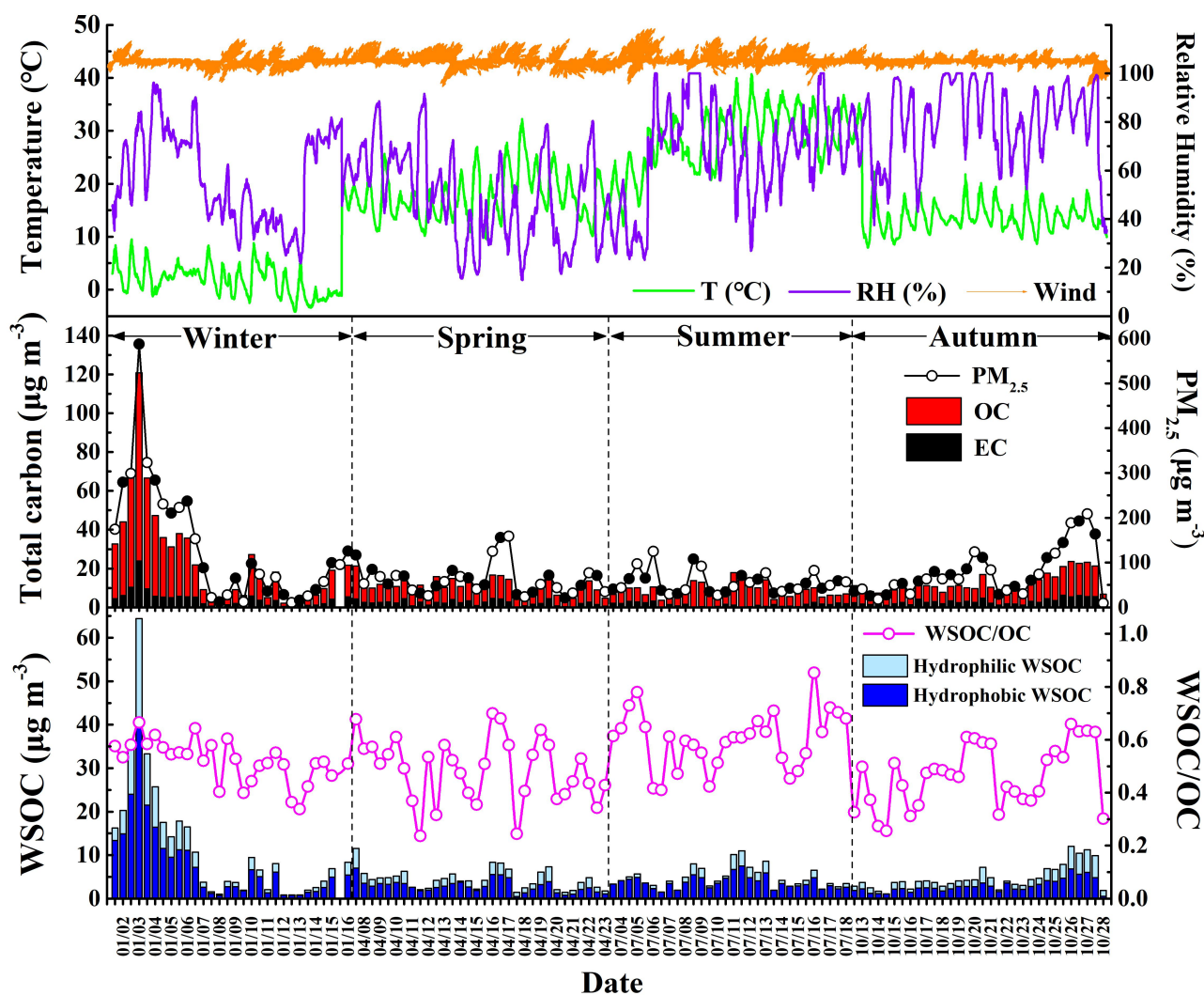


Figure 1. Temporal variations of meteorological parameters, mass concentrations of $PM_{2.5}$, OC, EC, WSOC and WSOC/OC ratio in Beijing during the sampling periods in different seasons of 2017.

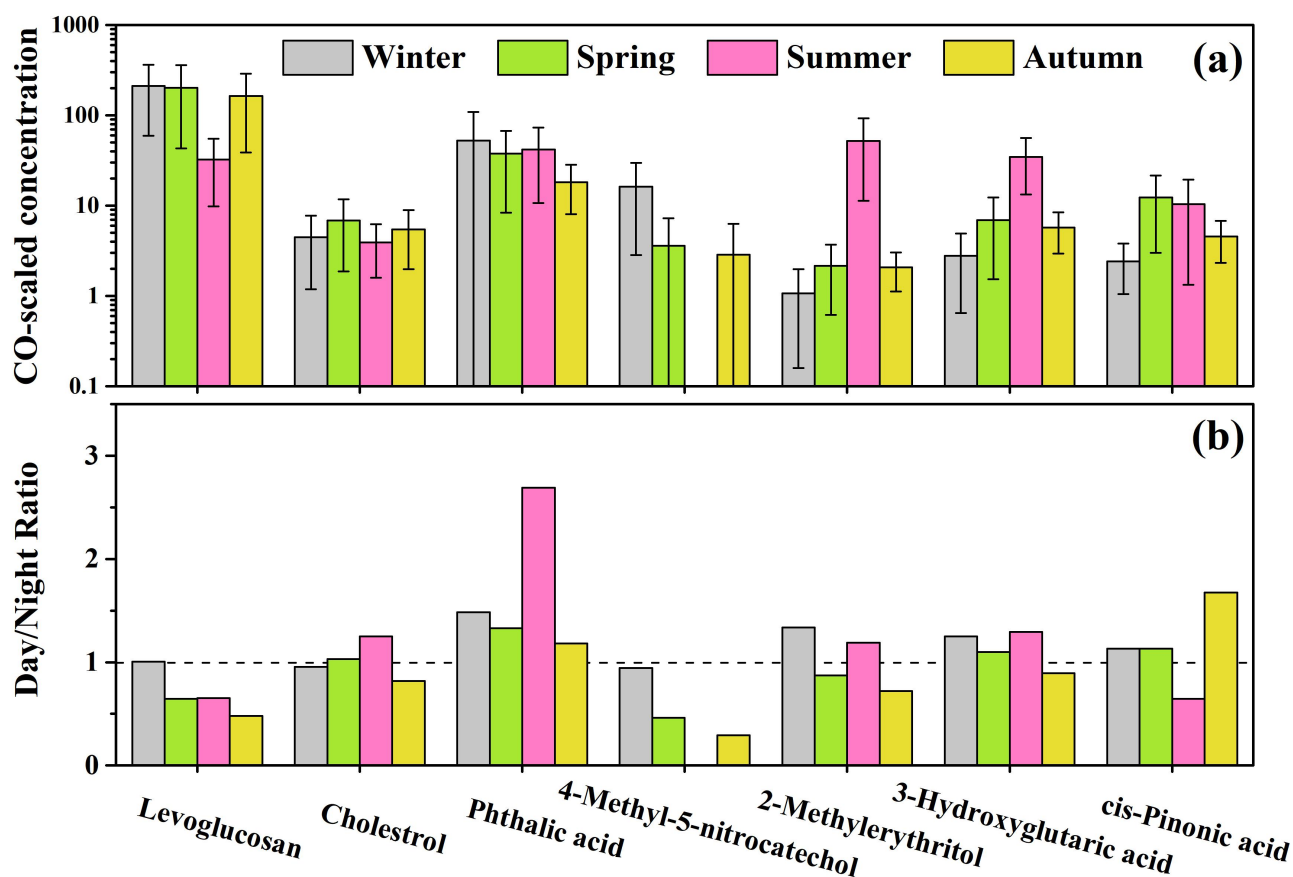


Figure 2. Seasonal variations and diurnal patterns of the identified organic tracers in Beijing during the sampling periods in four seasons of 2017.

850

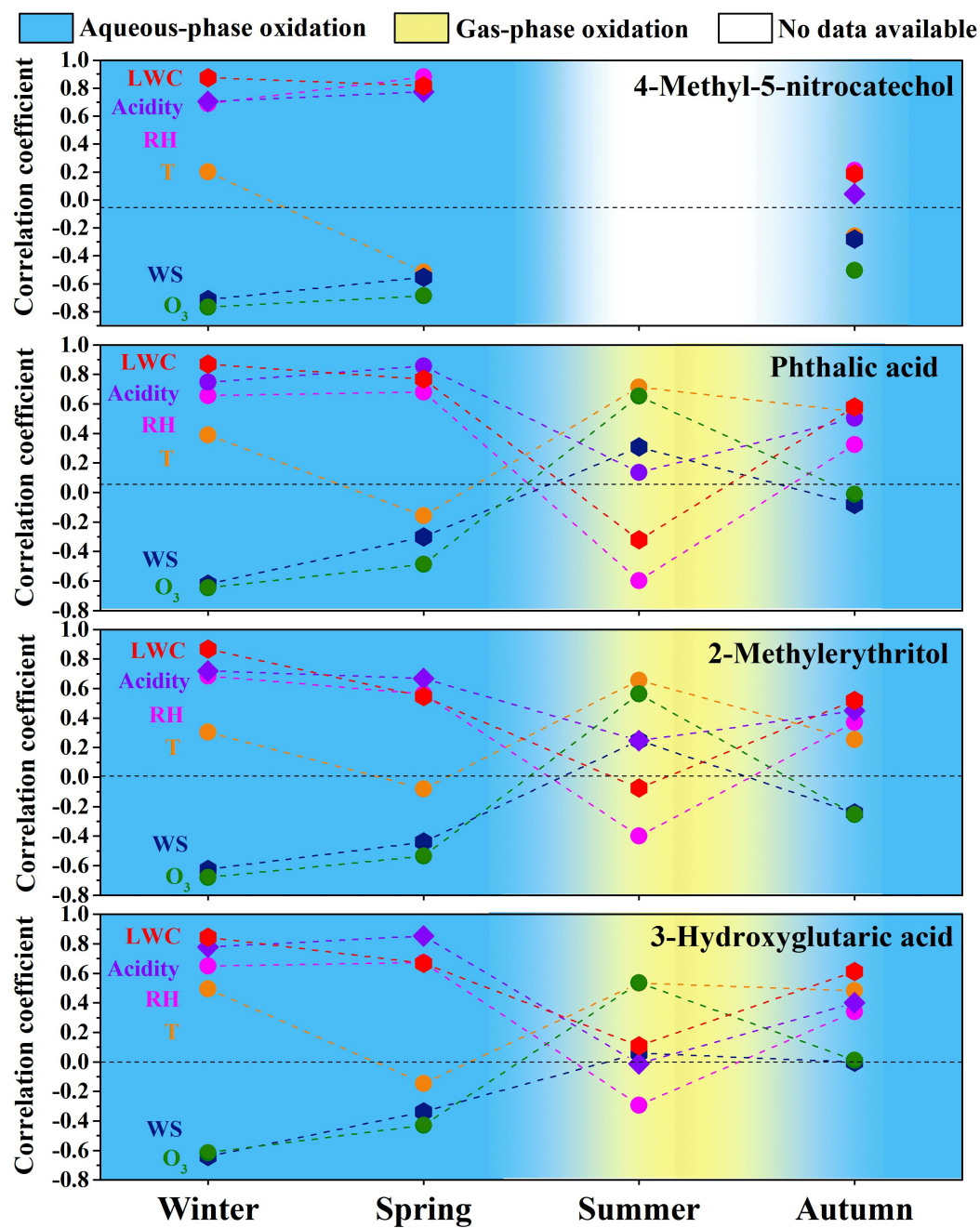
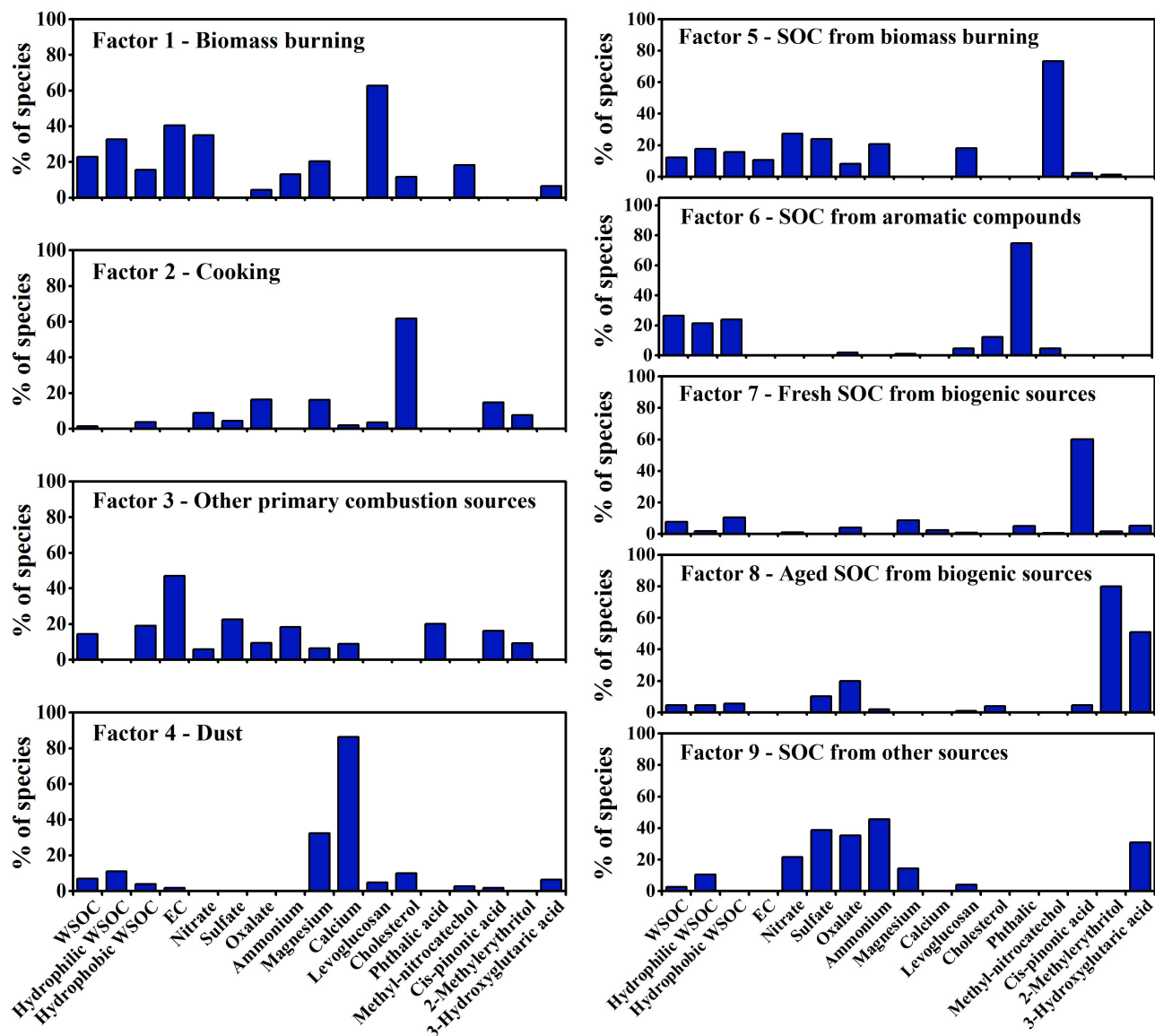


Figure 3. Correlation coefficients between the identified SOA tracers and the meteorological parameters, O₃ concentration, aerosol acidity and liquid water content (LWC) in four seasons of 2017.



860 **Figure 4.** Source profiles of WSOC in PM_{2.5} resolved by the PMF model.

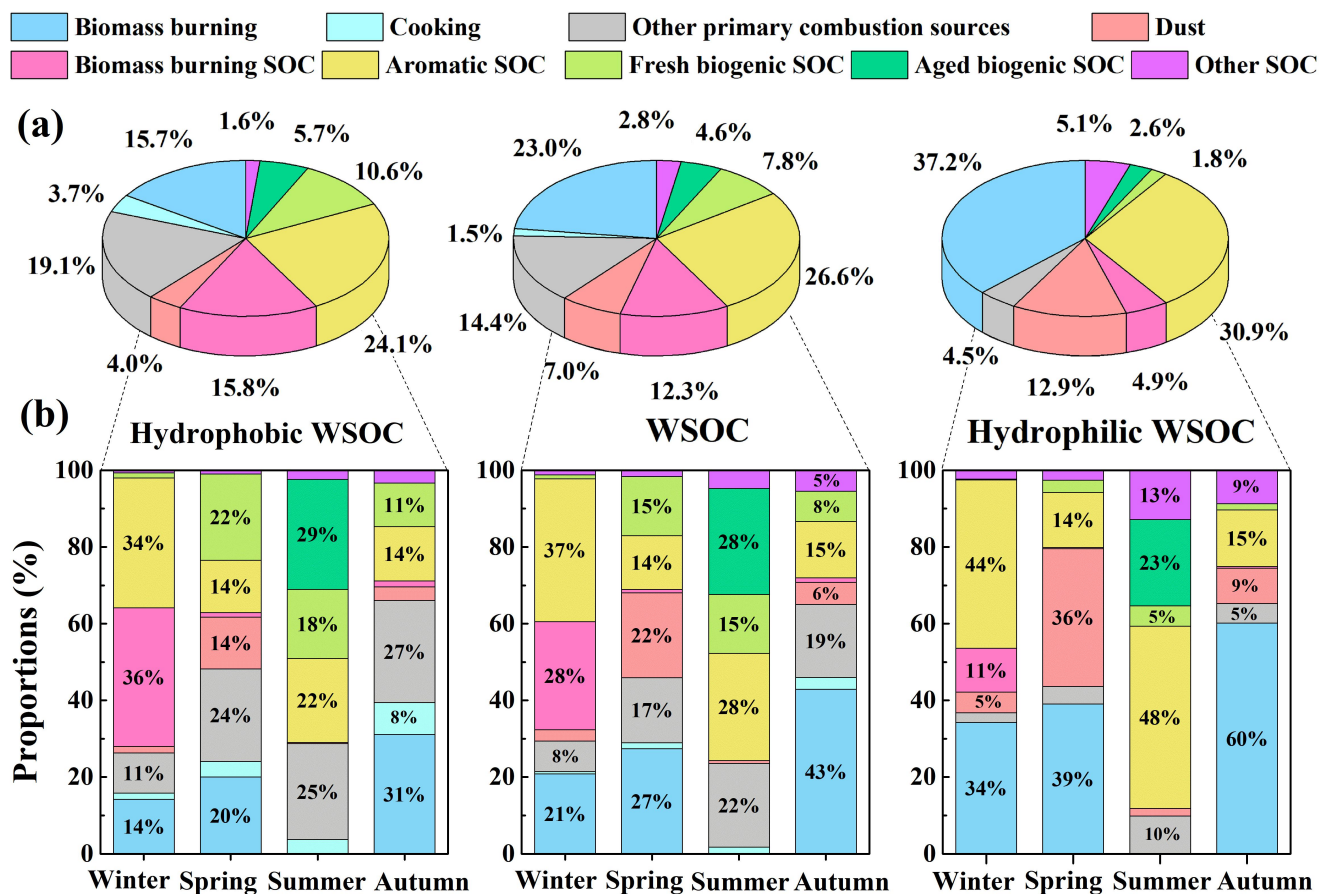
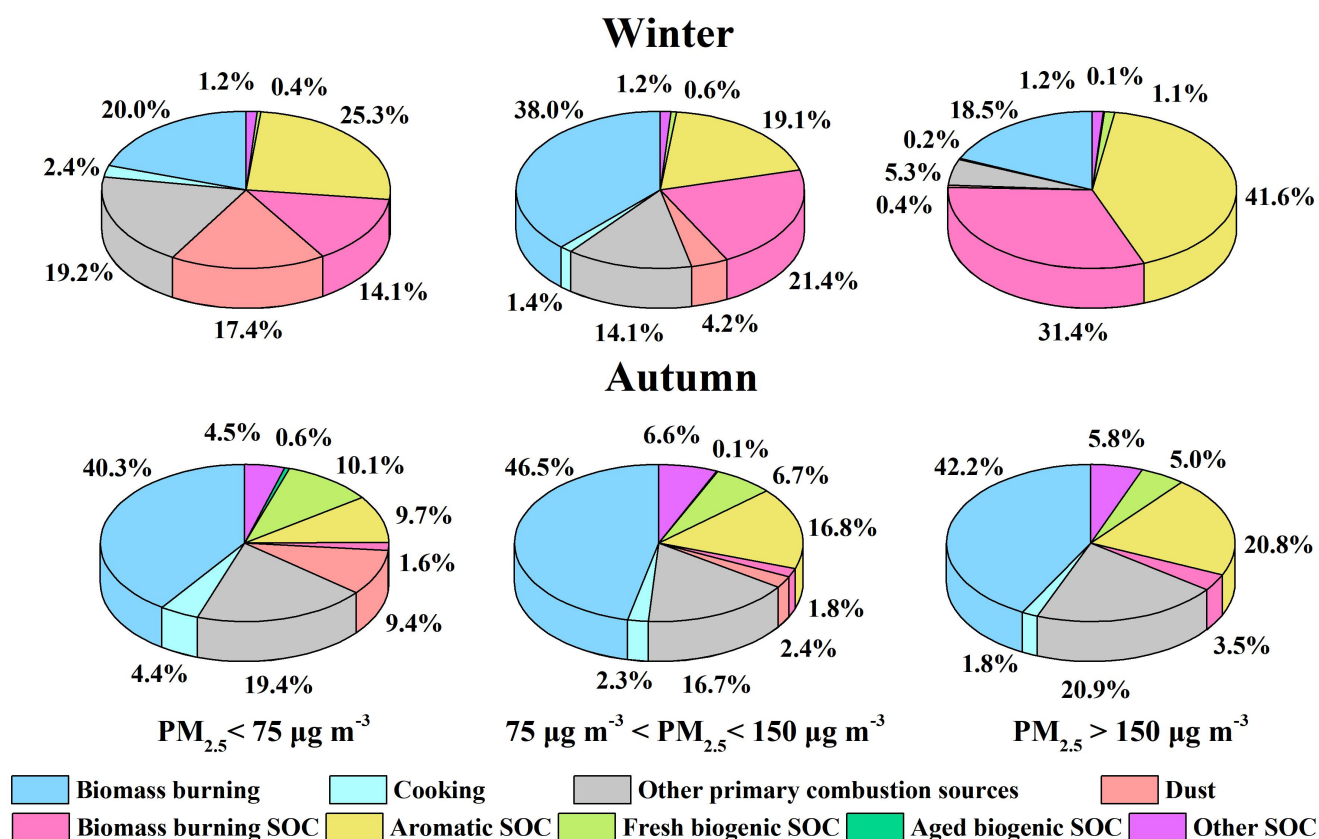


Figure 5. Source contributions of WSOC as well as its hydrophobic and hydrophilic fractions in Beijing: (a) comparison of the source contributions to total WSOC, hydrophobic WSOC and hydrophilic WSOC on the whole year scale; (b) seasonal variations of the source contributions to total, hydrophobic and hydrophilic WSOC in different seasons.



870 **Figure 6.** Source contributions to WSOC in PM_{2.5} at different pollution levels in winter and autumn.

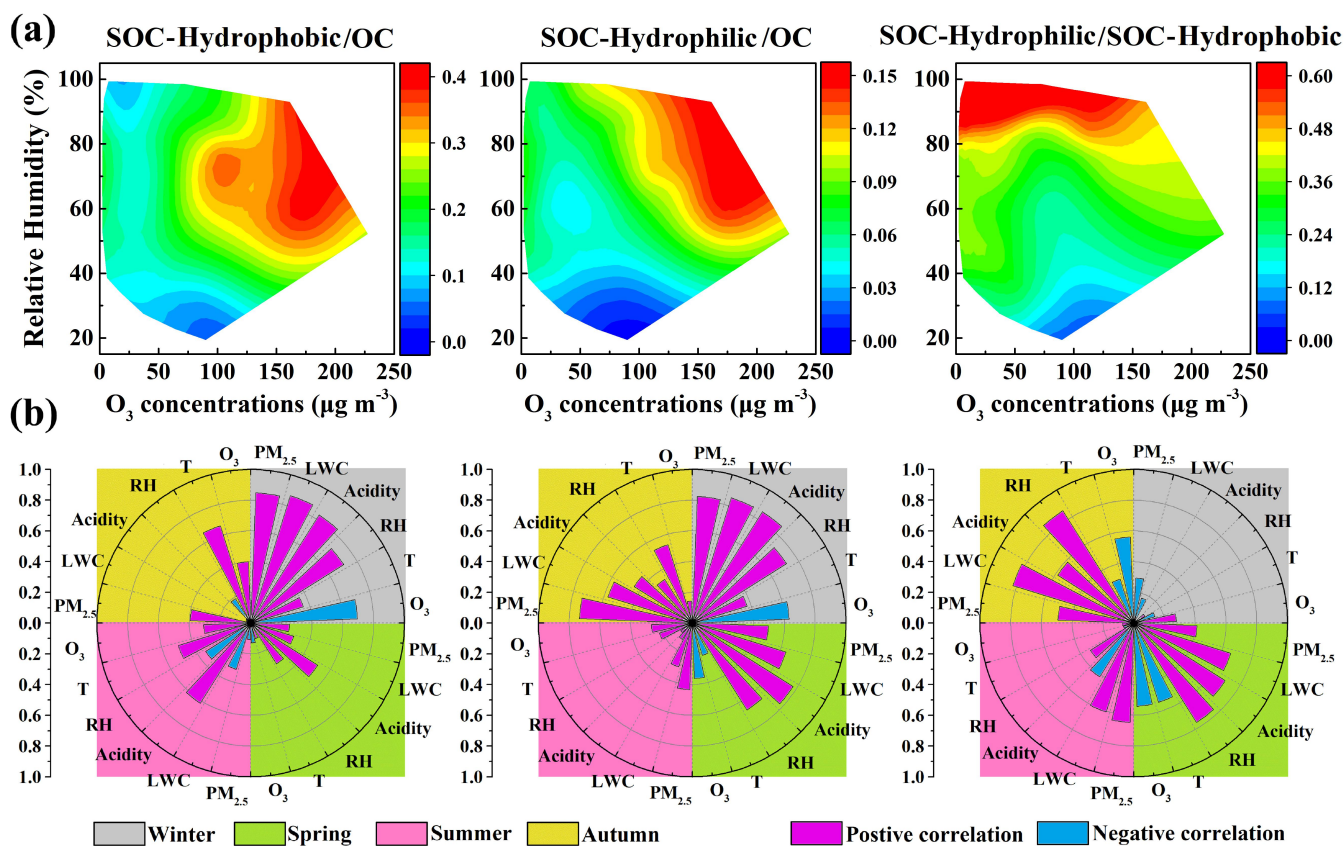


Figure 7. The RH versus O₃ dependence of hydrophobic SOC/OC, hydrophilic SOC/OC and hydrophilic SOC/ hydrophobic SOC ratios over the whole sampling period (a), and the correlation coefficients between the above ratios and meteorological parameters, O₃, PM_{2.5}, aerosol acidity and liquid water content (LWC) in the four seasons (b).